Porphyrin Sponges: Conservation of Host Structure in over 200 Porphyrin-Based Lattice Clathrates

Marianne P. Byrn, Carol J. Curtis, Yu Hsiou, Saeed I. Khan, Philip A. Sawin, S. Kathleen Tendick, Aris Terzis,† and Charles E. Strouse*

Contribution from the Department of Chemistry and Biochemistry, University of California, Los Angeles, California 90024-1569, and Institute of Materials Science, N.R.C. "Demokritos", Ag. Paraskevi 15310, Athens, Greece

Received March 11, 1993®

Abstract: Analysis of the molecular packing in over 200 tetraarylporphyrin-based lattice clathrates reveals a strong conservation of host structure. In most cases, formation of porphyrin-based clathrates can be viewed as arising from intercalation of guest molecules into pure host materials. Several modes of intercalation are detected, and characteristic of intercalate structures, staging is observed. Intercalate formation accounts for the relative insensitivity of the host structure to the nature and size of the guest species. The structural conservation observed in this large class of materials facilitates rational modification of the host lattice. Crystallographic data are provided for 75 new porphyrin-based clathrates.

Introduction

Tetraarylporphyrin molecules are remarkably versatile building blocks for the construction of clathrate lattices. Porphyrin-based host lattices are capable of accommodating an extremely wide range of guest species. The driving force for guest incorporation is the fact that the large, rigid, highly-symmetric host molecules cannot pack efficiently in three dimensions. The introduction of guest molecules into the crystalline lattice provides the degrees of freedom necessary to achieve more efficient packing.

Tetraarylporphyrins are particularly useful host materials because of the strong conservation of host structure in the clathrates that they form. Previous reports from this laboratory[1] described approximately 100 "porphyrin sponges" in which corrugated sheets of porphyrin molecules, very similar to those seen in pure host materials, are separated by sheets of guest molecules. These materials can best be described as stage 1 intercalates.[2] The conservation of the porphyrin sheet structure, along with the fact that the guest sites in these clathrates coincide with the axial coordination sites of the porphyrin metal atoms, suggested a new approach to the rational design of microporous solids. Earlier reports outlined this approach and demonstrated the feasibility of a variety of technological applications.

Recent efforts designed to exploit the "programmability" of porphyrin-based hosts have involved the preparation and characterization of many new materials and have generated a large base of structural data. Analysis of this rapidly expanding database has revealed a larger and more diverse class of porphyrin-based intercalates. The goal of this report is to provide a detailed description of the structural relationships among these materials. The analysis presented involves the transformation of related

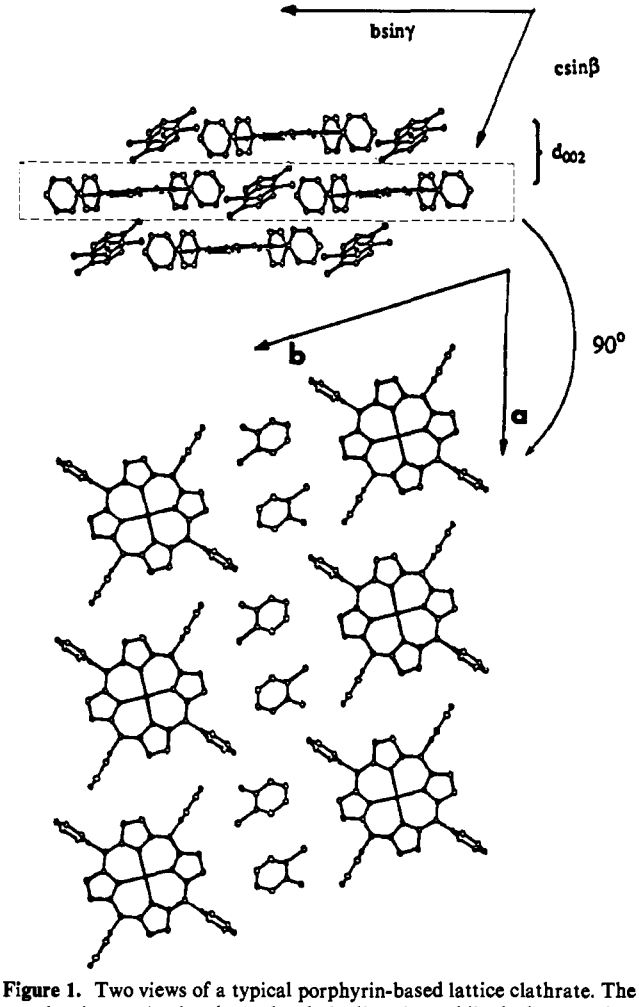

Figure 1. Two views of a typical porphyrin-based lattice clathrate. The top view is a projection down the chain direction, while the bottom view shows a section through the channel.

* Address correspondence to this author at the University of California, Los Angeles.
† "Demokritos", Athens, Greece
® Abstract published in *Advance ACS Abstracts*, September 1, 1993.

(1) (a) Byrn, M. P.; Curtis, C. J.; Khan, S. I.; Sawin, P. A.; Tsurumi, R.; Strouse, C. E. *J. Am. Chem. Soc.* **1990**, *112*, 1865–1874. (b) Byrn, M. P.; Strouse, C. E. *J. Am. Chem. Soc.* **1991**, *113*, 2501–2508. (c) Byrn, M. P.; Curtis, C. J.; Goldberg, I.; Hsiou, Y.; Khan, S. I.; Sawin, P. A.; Tendick, S. K.; Strouse, C. E. *J. Am. Chem. Soc.* **1991**, *113*, 6549–6557. (d) Byrn, M. P.; Curtis, C. J.; Goldberg, I.; Huang, T.; Hsiou, Y.; Khan, S. I.; Sawin, P. A.; Tendick, S. K.; Terzis, A.; Strouse, C. E. *Mol. Cryst. Liq. Cryst.* **1992**, *211*, 135–140.

(2) The terms "lattice clathrate" and "clathrate" are used herein in the most general sense to indicate the inclusion of "guest" molecules in a crystalline lattice of "host" molecules. No distinction is made for those cases in which there is a strong specific interaction between host and guest molecules. Similarly, the term "intercalate" is used to indicate the observation of two-dimensional structure similar to that observed in pure host materials. The use of this term is not intended to indicate knowledge of the *mechanism* of clathrate formation.

0002-7863/93/1515-9480$04.00/0

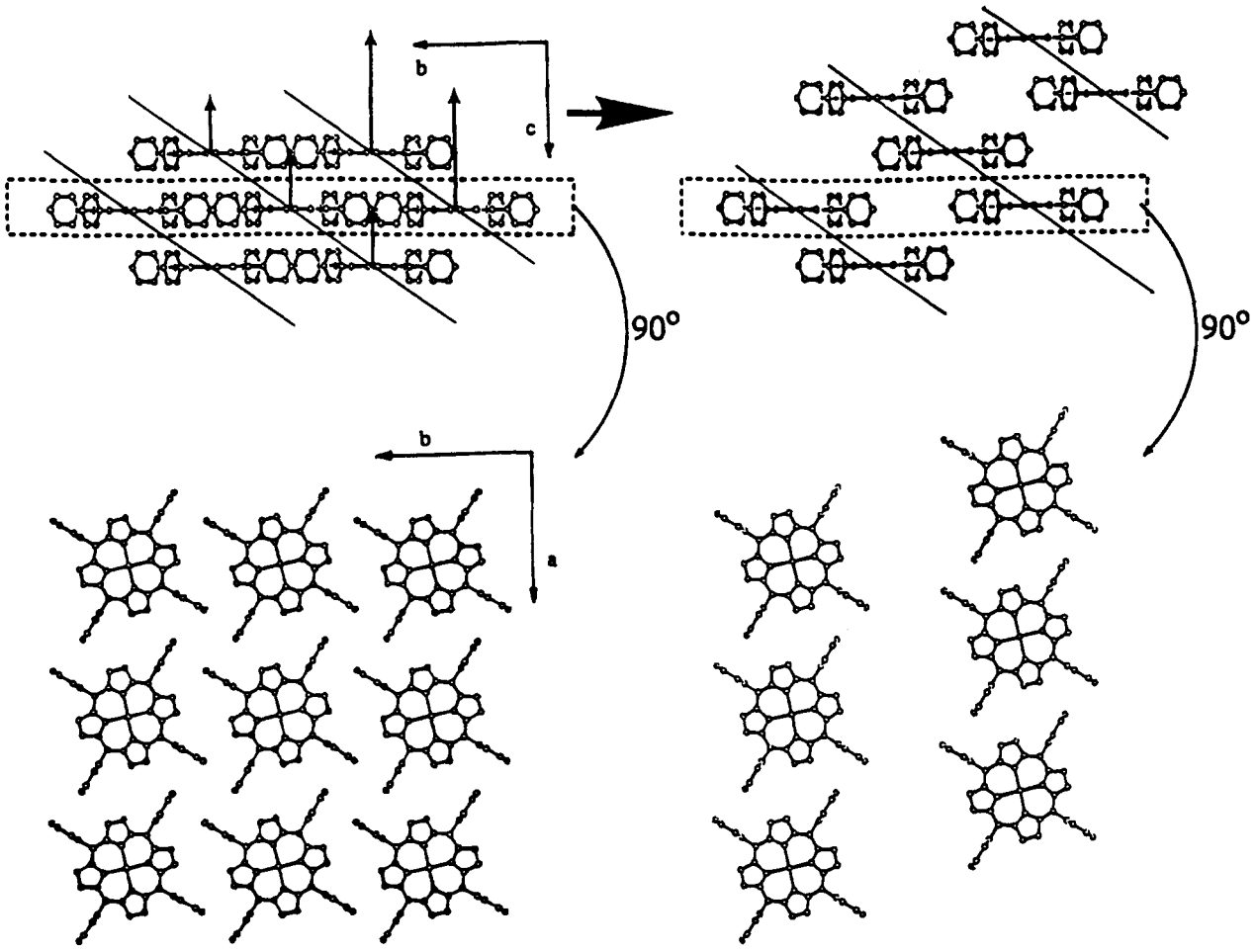

Figure 2. Relationship between the I4/m host structure[7] and that of a "normal" triclinic clathrate.

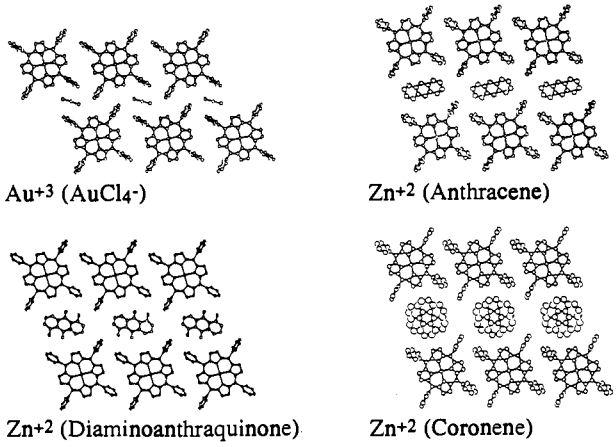

Figure 3. "Normal" porphyrin-based clathrates with a single centrosymmetric guest molecule per porphyrin molecule.

crystal structures to a common crystallographic coordinate system and the description of the clathrate structures in terms of shear distortions of two basic host structures. Reported herein are analyses of 142 porphyrin-based clathrates not discussed in earlier reports, including 87 based on new structure determinations. Crystallographic data are provided for 75 new materials; the data for the remaining 12 will be reported elsewhere. The structural relationships revealed in this investigation, along with the large body of new experimental data, promise to be of value both in the application of porphyrin-based clathrates and more generally in the designed construction of new molecular solids.

Experimental Section

X-ray Measurements. All X-ray measurements made use of locally automated Huber, Syntex, and Picker diffractometers equipped with graphite monochromatized Mo and Cu sources. The Huber diffractometer is equipped with a closed cycle Air Products refrigerator, and the Picker diffractometer is equipped with a gas stream low-temperature device. All crystals were coated with epoxy or grease to prevent loss of solvate and mounted on glass fibers. Crystallographic techniques used have been described previously.[1b]

Table I. Crystallographic Symmetry of Porphyrin-Based Lattice Clathrates for Which X-ray Structural Data Are Available[a]

crystal symmetry	Z	number	crystal symmetry	Z	number
triclinic	1	139	tetragonal	2	20
	2	81		4	9
monoclinic	2	56		8	3
	4	132	rhombohedral	6	3
	8	10	total		480
orthorhombic	2	1			
	4	18			
	8	8			

[a] These materials include 352 taken from the January 1992 version of the Cambridge Structural Database,[3] 34 reported in a previous paper in this series,[1c] and 94 previously unpublished structures determined in this laboratory. Dimeric or heavily substituted porphyrins from the database were not included in this count.

Synthesis. In most cases, clathrates were prepared by recrystallization of the host from liquid guest. For high-melting guests, crystals were formed by cooling solutions of the host and guest in mesitylene, *p*-diisopropylbenzene, 1,3,5-triisopropylbenzene, chloroform, or benzene (Aldrich Chemical). Fe(III) tetraphenylporphyrin (TPP) phenolate complexes were prepared by the reaction of $(FeTTP)_2O$ and the appropriate phenol in refluxing benzene. The monoclinic form of ZnTPP was prepared by crystallizing ZnTPP from 1,3,5-triisopropylbenzene at elevated temperature. Tetraphenylporphyrin was prepared by the condensation of pyrrole and benzaldehyde in refluxing propionic acid. Zinc tetraphenylporphyrin was prepared by the reaction of tetraphe-

Table II. Triclinic Z = 1 Tetraphenylporphyrin-Based Lattice Clathrates[a]

metal	guest	a	b	c	α	β	γ	vol	d(002)	ref	figure
		a. "Normal" Clathrates									
Zn^{+2}	(4-nitropicoline *N*-oxide)	13.409	18.320	13.992	60.71	41.93	80.21	(1889)	3.902	this work	4
Fe^{+3}	(3-acetylphenolate$^-$)	13.466	17.858	14.068	61.02	42.51	80.57	(1890)	3.983	this work	4
Au^{+3}	($AuCl_4^-$)	13.796	17.718	17.676	54.41	34.34	55.11	1942	4.844	FUJFEV[8]	3
Mg^{+2}	(pyridine)$_2$	13.374	17.869	12.612	65.15	49.98	75.56	2094	4.523	this work	5
Zn^{+2}	(anthracene)	13.423	19.122	13.007	60.01	47.51	75.65	2111	4.245	this work	3
Fe^{+3}	(phenolate$^-$)(benzene)	13.519	19.377	12.121	58.37	51.52	71.63	(2116)	4.256	this work	6
Zn^{+2}	(1,5-diaminoanthraquinone)	13.410	20.344	11.644	60.23	50.26	71.08	(2120)	4.108	this work	3
Zn^{+2}	(aniline)$_2$	13.608	20.237	11.672	58.16	52.74	71.04	(2173)	4.172	this work	5
Zn^{+2}	(phenyl isocyanate)$_2$	13.661	20.414	12.589	57.59	47.83	71.12	(2193)	4.155	this work	5
Zn^{+2}	(benzacephenanthrylene)	13.438	21.078	12.161	61.01	47.48	72.33	(2219)	4.112	this work	4
Zn^{+2}	(2,3-benzofluorene)	13.514	20.883	11.527	64.36	49.28	73.60	2223	4.105	this work	4
Zn^{+2}	(1,2-benzanthracene)	13.489	20.996	11.651	63.14	49.17	73.07	2228	4.111	this work	4
Zn^{+2}	(methoxypyrazine)$_2$	13.422	17.715	10.962	79.30	61.65	79.66	2241	4.791	this work	5
Fe^{+3}	(phenolate$^-$)(toluene)	13.540	19.737	11.934	58.89	55.70	71.44	2254	4.449	this work	6
Zn^{+2}	(anisole)$_2$	13.408	21.605	11.361	63.05	50.50	74.38	2263	4.056	this work	5
Zn^{+2}	(2-fluorotoluene)$_2$	13.555	21.709	11.386	64.12	48.74	74.22	2265	4.000	this work	5
Pd^{+2}	*N,N'*-(benzyloxy)methylene (Br^-)$_2$ (CH_2Cl_2)	13.357	22.053	10.591	68.22	51.54	75.92	2268	3.970	BESFOU[9]	6
Zn^{+2}	(*o*-toluic aniline)$_2$	13.697	19.771	11.783	58.38	56.68	72.28	2270	4.400	this work	5
Zn^{+2}	(indole)$_2$	13.627	21.702	11.049	64.89	50.42	71.95	2277	4.049	this work	5
Zn^{+2}	(anthranilonitrile)$_2$	13.693	20.664	11.942	57.46	53.50	69.32	2287	4.320	this work	5
Fe^{+3}	(2-chlorophenolate$^-$)(*m*-xylene)	13.501	20.020	11.710	58.97	57.76	71.75	2291	4.462	this work	6
Zn^{+2}	(indene)$_2$	13.633	22.033	11.162	65.54	49.08	73.10	2305	4.010	this work	5
Zn^{+2}	(2-acetylpyridine)$_2$	13.440	20.141	12.238	54.72	58.55	72.25	2307	4.474	this work	5
Zn^{+2}	(3-methyl-2-cyclohexenone)$_2$	13.504	18.920	11.652	64.14	60.48	72.96	2319	4.748	10	6
Zn^{+2}	(2-chloro-4,5-dimethylphenol)$_2$	13.762	20.487	11.737	53.87	60.44	72.59	(2325)	4.321	this work	5
Zn^{+2}	(2-nitro-4-cresol)$_2$	13.643	20.319	11.626	56.46	60.77	74.64	2344	4.385	this work	5
Zn^{+2}	(α-methylstyrene)$_2$	13.638	21.996	11.604	65.43	47.87	74.25	2348	4.066	this work	5
Zn^{+2}	(coronene)	13.198	21.625	13.174	60.61	46.88	74.89	2375	4.309	this work	3
Zn^{+2}	(benzenechromium-$(CO)_3$)$_2$	13.346	18.679	11.542	78.15	63.53	78.26	2500	5.122	this work	5
Zn^{+2}	(1,7-spiroacetal)$_2$	13.223	23.637	10.594	79.72	52.58	75.09	2540	4.205	10	5
hypothetical[b]		13.440	21.251	13.590	51.28	60.37	71.57	2632	4.857		
		b. "Double-Row" Clathrates									
Zn^{+2}	(2,4,5-trichlorophenol)$_2$	13.046	24.963	18.126	41.85	41.38	70.00	(2267)	3.703	this work	
Zn^{+2}	(4-vinylanisole)$_2$	13.410	26.877	17.639	40.51	38.30	62.68	2405	3.756	this work	
Zn^{+2}	(2-OH-4-MeO-acetophenone)$_2$	13.627	25.228	20.375	41.93	37.35	66.89	2474	3.913	this work	
Zn^{+2}	(4-phenyl-3-buten-2-one)$_2$	13.446	27.227	17.193	38.76	41.47	62.43	2495	3.844	this work	
Zn^{+2}	(phenazine)$_2$	13.322	27.945	16.661	39.56	42.71	65.84	2496	3.674	this work	
Zn^{+2}	(bianthrone)	13.451	22.353	20.784	45.18	37.29	65.07	(2540)	4.658	this work	
Fe^{+3}	$(ImH)_2(Cu^{+3}(mnt^{-2})_2)(THF)_4$	13.723	26.120	18.358	39.70	56.83	73.23	(3408)	4.965	KEHYIF[11]	
		c. "Expanded a" Clathrates									
Zn^{+2}	(tetramethyl pyromellitate)	14.874	23.056	11.975	58.66	42.81	58.54	2313	3.953	this work	
Zn^{+2}	(Cu^{+2}(2,4-pentadionate$^-$)$_2$)	14.860	24.459	11.644	54.62	41.38	57.46	2238	3.653	this work	
Zn^{+2}	(2-nitrobenzaldehyde)$_2$	16.498	24.009	13.841	45.33	36.19	61.71	(2245)	3.218	this work	
Zn^{+2}	(terephthaldicarboxaldehyde)$_2$	15.943	24.670	13.830	46.54	35.94	60.73	2288	3.334	this work	
$2H^+$	[T(C_6F_5)P](dioxane)$_2$	16.137	16.957	25.820	56.97	24.99	58.80	2497	5.334	this work	
hypothetical		15.018	26.247	16.899	43.39	34.57	52.52	2596	4.149		
		d. "*mmm*" Clathrates									
Zn^{+2}	(eugenol)$_2$	16.837	21.636	16.051	60.01	31.06	67.22	2602	3.874	10	
hypothetical		14.795	25.133	20.465	57.25	25.94	64.05	2774	4.149		
		e. "Layered Clathrates"									
Zn^{+2}	(9,10-diphenethynylanthracene)	13.022	17.285	13.132	86.38	88.14	58.57	(2517)	6.553	this work	

[a] The body-centered unit cell chosen to describe these materials is the same as that used previously.[1a,c] This unit cell contains two porphyrin molecules per unit cell. The Z = 1 designation used in this report refers to one porphyrin molecule in the *primitive* unit cell. A cell volume in parentheses indicates that data were collected at low temperature. For those structures taken from the Cambridge Structural Database, the refcode is provided. Unless otherwise noted, the porphyrin is tetraphenylporphyrin. [b] The β reported for this hypothetical cell in an earlier publication[1c] was incorrect.

nylporphyrin with zinc acetate in refluxing dimethylformamide. Other porphyrins were obtained from Midcentury Chemical (Posen, IL).

Results

The "isostructural" porphyrin-based clathrates described in previous reports[1a-c] from this laboratory contain one porphyrin molecule in the primitive triclinic unit cell (Z = 1). While this packing motif is the most common for tetraphenylporphyrin-based clathrates, the breakdown in Table I reveals significant numbers of triclinic Z = 2, monoclinic, and tetragonal materials. The relationships among the triclinic Z = 1 and tetragonal structures were discussed previously.[1a,c] In the present report, the analysis of structural systematics is extended to reveal some striking similarities in the host structures of the triclinic Z = 1, the triclinic Z = 2, and the monoclinic clathrates.

Triclinic Z = 1 Clathrates. Figure 1 shows two views of a typical triclinic Z = 1 clathrate. The guest species in these clathrates occupy channels that are bounded by four chains of porphyrin molecules. These chains are stacked stepwise to form corrugated sheets parallel to the (0,1,1) family of planes. Sheets of porphyrin molecules alternate with sheets of guest species to form a stage 1 intercalate. The porphyrin chains are characterized by a perpendicular arrangement of interacting phenyl groups and by a repeat distance of about 13.5 Å. This chain structure is the most common of several identified previously and is referred to herein as the "normal" structure. The interaction between phenyl groups on adjacent molecules of a chain is similar to that seen in solid benzene.[4] The stabilization associated with this type of interaction has been examined.[5] Stacking of chains in a

(3) Allen, F. H.; Kennard, O.; Taylor, R. *Acc. Chem. Res.* **1983**, *16*, 146–153.

(4) (a) Bacon, B. E.; Curry, N. A.; Wilson, S. A. *Proc. R. Soc. London, A* **1964**, *279*, 98–110. (b) Williams, D. E. *Acta Crystallogr.* **1980**, *A36*, 715–723.

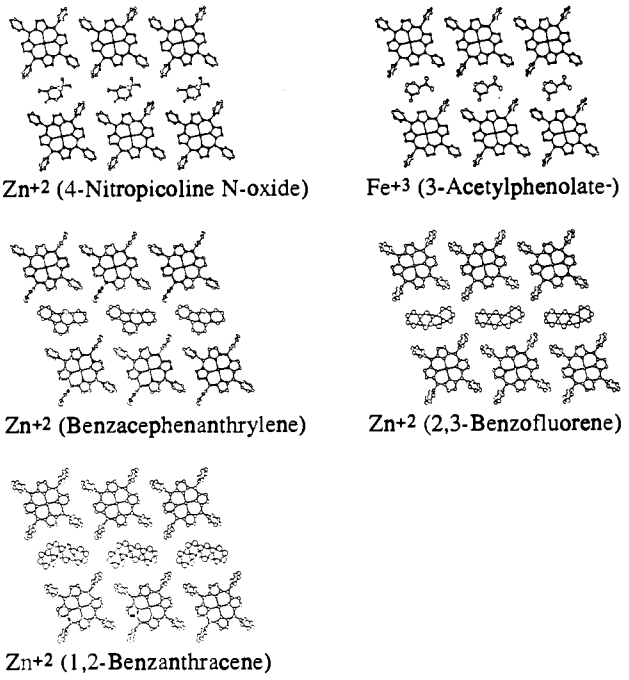

Figure 4. "Normal" clathrates with a single non-centrosymmetric guest molecule per porphyrin molecule. In all these clathrates, the guest molecules exhibit inversion disorder; the figures depict the guest molecule in one of two possible dispositions. Order and twinning parameters[1b] were used to model the inversion disorder. In most cases the order parameter was found to be significantly different from zero, i.e., there is significant residual order.

porphyrin sheet should produce a similar stabilization, since the phenyl groups of one chain interact in a perpendicular fashion with the porphyrin cores of adjacent chains.

The "normal" porphyrin clathrate lattice can be described as resulting from a shear distortion of the I4/m host structure exhibited by a number of tetraphenylporphyrin complexes containing very small axial ligands (e.g. ZnTPP(H_2O)[6]). The distortion occurs along (0,1,1) shear planes (see Figure 2) to yield a layer of open channels between adjacent porphyrin sheets. This space is occupied by the guest molecules. The dimensions of the hypothetical unit cell resulting from a $c/2$ displacement

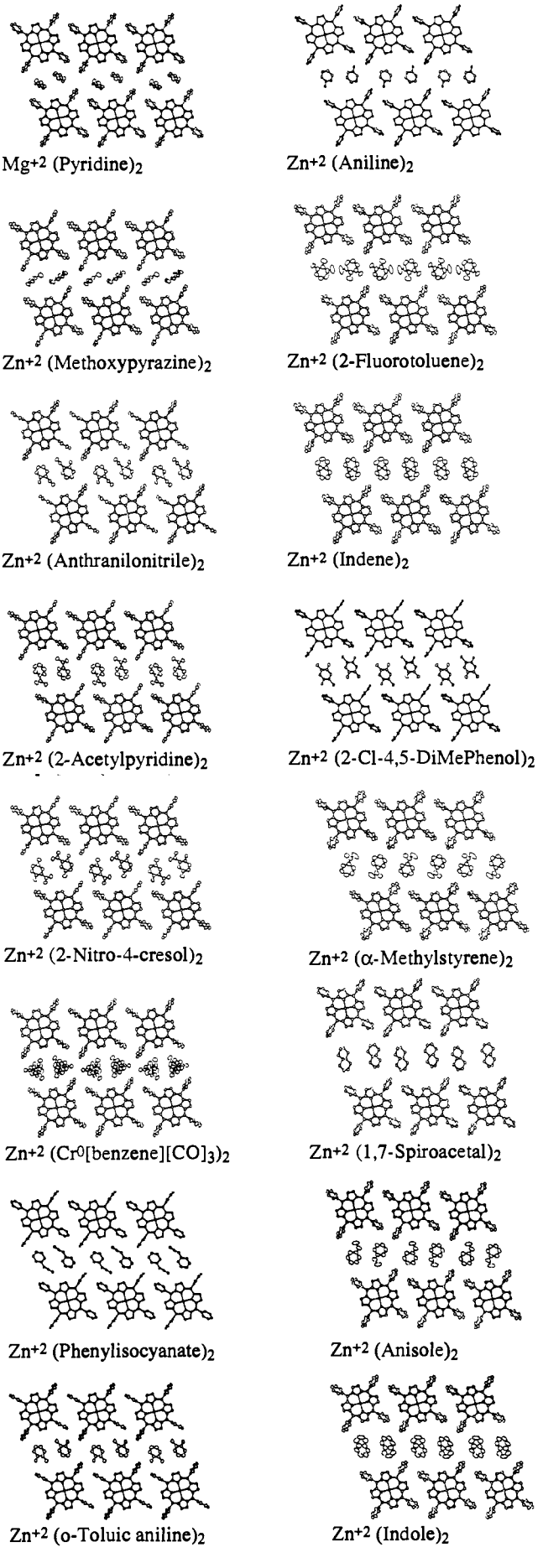

Figure 5. "Normal" clathrates with a guest/host ratio of 2:1. In the 2-fluorotoluene clathrate, the guest molecule is two-fold disordered.

(5) Jorgensen, W. L.; Severance, D. L. *J. Am. Chem. Soc.* **1990**, *112*, 4768–4774.

(6) Abbreviations used herein: acac, 2,4-pentanedionate; AcPH, acetophenone; bicycloheptene-CO_2^-, bicyclo[2.2.1]heptene-2-carboxylate; CC(phenyl)(4-chlorophenyl), (phenyl)(4-chlorophenyl)vinylidenecarbene; Et, ethyl; grandlure II, (*Z*)-3,3-dimethyl-Δ-1,α-cyclohexaneethanol; grandlure III, (*Z*)-3,3-dimethyl-Δ-1,α-cyclohexaneacetaldehyde; grandlure IV, (*E*)-3,3-dimethyl-Δ-1,β-cyclohexaneacetaldehyde; ImH, imidazole; Me, methyl; MeIm$^-$, methylimidazolate; mnt^{-2}, *cis*-dicyanoethylenedithiolate; $Na^+\subset$dibenzo-18-crown-6, sodium cryptate of dibenzo-18-crown-6; $Na^+\subset$222, sodium cryptate of 4,7,13,16,21,24-hexaoxa-1,10-diazabicyclo[8.8.8]hexacosane; (*o*-NH_2)TPP, (*o*-aminophenyl)(trisphenyl)porphinato; *N*-benzTPP, *N*-benzyltetraphenylporphinato; *N*-:CCOOEtTPP, *N*-((ethoxycarbonyl)carbene)tetraphenylporphinato; *N*-MeTPP, *N*-methyltetraphenylporphinato; [*N*,*N*'-CObenz], *N*,*N*'-((benzyloxy)methylene)tetraphenylporphyrin; *N*-tosylaminoTPP, *N*-(tosylamino)tetraphenylporphinato; Ph, phenyl; PMS, pentamethylene sulfide; 1,7-spiroacetal, 1,7-dioxaspiro[5,5]undecane; THF, tetrahydrofuran; T(*p*-MeO)P, tetrakis(*p*-methoxyphenyl)porphinato; TTP, tetratolylporphinato; TPB, tetraphenylbacteriochlorinato; TPC, tetraphenylchlorinato; TDCPP, tetrakis(2,6-dichlorophenyl)porphinato; TOPP, tetrakis(4-*n*-octylphenyl)porphinato; TOOPP, tetrakis(4-oxy-*n*-octyl)phenylporphinato; T(4-OH)PP, tetrakis(4-hydroxyphenyl)porphinato; TPpivP, tetrakis(*o*-pivalamidophenyl)porphinato; T(C_6F_5)P, tetrakis(perfluorophenyl)porphinato.

(7) The structure shown in Figure 2 is based on that of ZnTPP(H_2O) (Glick, M. D.; Cohen, G. H.; Hoard, J. L. *J. Am. Chem. Soc.* **1967**, *89*, 1996–1998).

(8) Schacter, A. M.; Fleischer, E. B.; Haltiwanger, R. C. *Acta Crystallogr., Sect. C* **1987**, *43*, 1876–1878.

(9) Callot, H. J.; Fischer, J.; Weiss, R. *J. Am. Chem. Soc.* **1982**, *104*, 1272–1276.

(10) Byrn, M. P.; Curtis, C. J.; Hsiou, Y.; Khan, S. I.; Sawin, P. A.; Terzis, A.; Strouse, C. E., to be published.

(11) Serr, B. R.; Headford, C. E. L.; Elliott, C. M.; Anderson, O. P. *Acta Crystallogr., Sect. C* **1990**, *46*, 500–502.

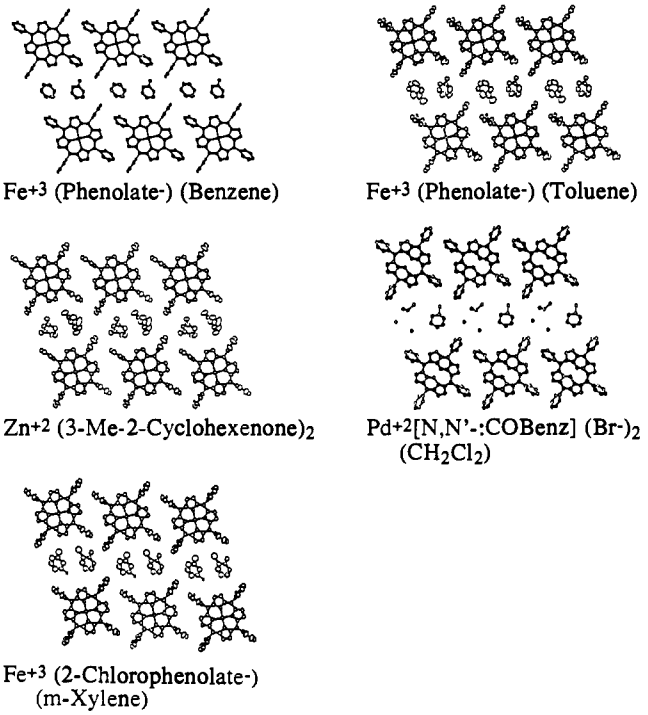

Figure 6. "Normal" clathrates with different species in adjacent guest sites. Inversion disorder was modeled with the order and twinning parameters.[1b] The phenolate clathrates exhibit incomplete disorder. The 3-methyl-2-cyclohexenone and the *N,N'*-CObenz clathrates are completely ordered.

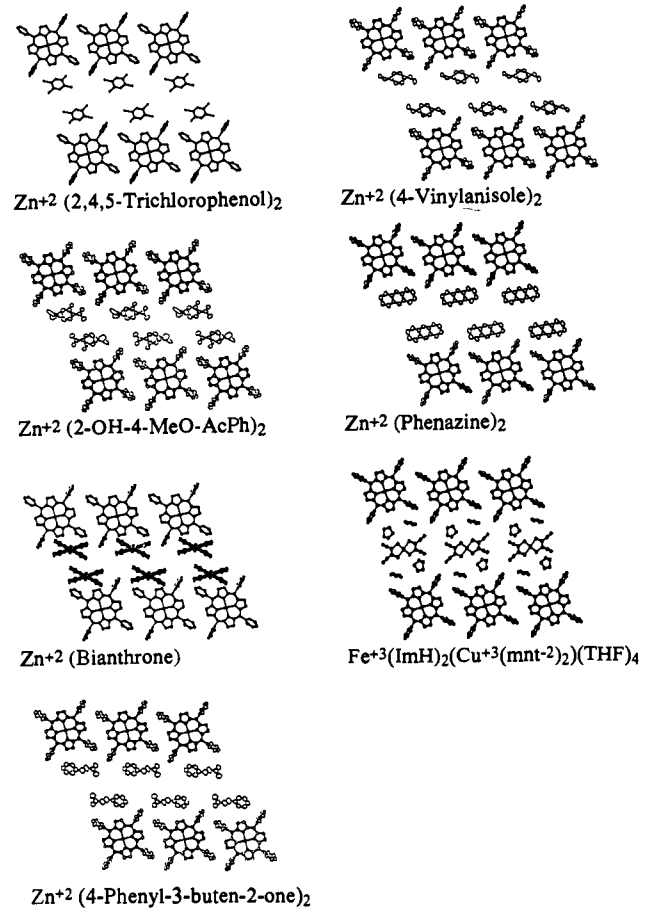

Figure 7. "Double-row" clathrates. The bianthrone clathrate has been included among those structures with the 2:1 stoichiometry because the single guest molecule occupies channel sites in two adjacent channels. Each anthrone moiety fills the role of a guest species.

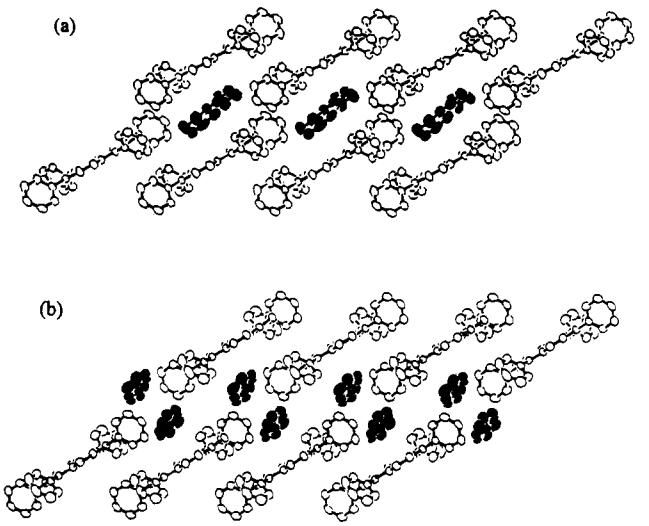

Figure 8. Comparison of the packing in "normal" and "double-row" clathrates viewed down the chain direction.

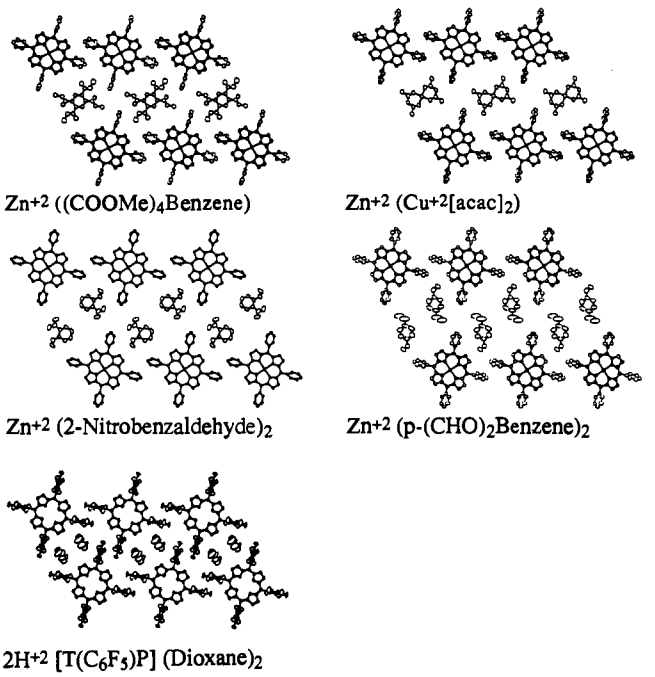

Figure 9. Clathrates with "expanded a" structures.

of (0,1,1) sheets correspond closely to the cell dimensions of "normal" triclinic clathrates (see Table IIa)

Figures 3–7 show crystal structures for 37 "normal" triclinic Z = 1 porphyrin clathrates not discussed in previous reports. Figure 3 depicts clathrates in which the guest/host ratio is 1:1 and a centrosymmetric molecule spans a crystallographic inversion center in the clathrate channel. Figure 4 shows clathrate structures in which the guest/host ratio is 1:1 but the guest molecule is non-centrosymmetric.

Figure 5 shows "normal" clathrates with two inversion related guest molecules per host molecule. The 2:1 guest/host stoichiometry is the most common for these porphyrin-based clathrates. The clathrates in Figure 6 have the same host structure but lack inversion symmetry.

Figure 7 shows clathrates in which the channel contains double rows of guest molecules. The lattice parameters for these materials can be found in Table IIb. Figure 8 shows a significant difference between the "normal" and "double-row" clathrates. In the "normal" structure, guest molecules in a channel are well isolated from those in adjacent channels. In the "double-row" materials, there are close contacts between guest molecules in adjacent channels.

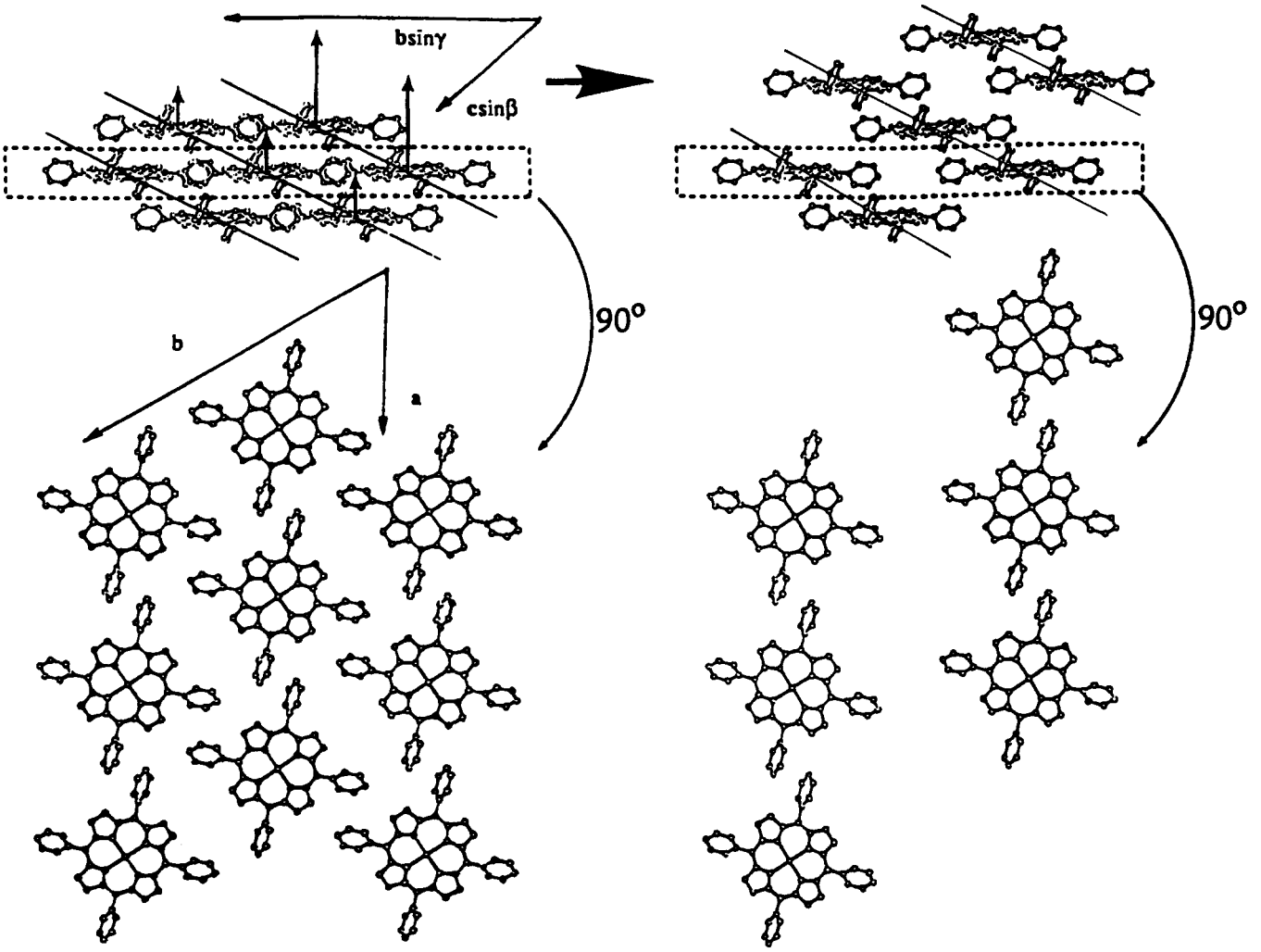

Figure 10. Relationship between the structures of pure triclinic ZnTPP and an "expanded a" clathrate. Adjacent sheets are shown separated along the normal to the *ab* plane by *d*(002).

Figure 9 shows clathrates that exhibit an "expanded a" structure. The porphyrin chains in these clathrate structures exhibit a parallel arrangement of nearest-neighbor phenyl groups and a repeat distance of about 15 Å. Lattice parameters for these clathrates are tabulated in Table IIc. The parallel stacking of phenyl groups in these materials is expected to provide some lattice stabilization.[5]

The "expanded a" clathrate lattice was previously described[1c] as resulting from a shear distortion of the "normal" clathrate structure. This lattice can also be described as resulting from intercalation of the guest species into a pure porphyrin lattice. The structure of a triclinic phase of ZnTPP has been determined[12] and exhibits chains and sheets of porphyrin molecules similar to those in the "expanded a" clathrates. Figure 10 depicts the transformation of the triclinic ZnTPP structure[13] to the "expanded a" clathrate structure. Displacement of (0,2,2) sheets along the normal to the *ab* plane by *d*(002) yields the open layer that accommodates the guest molecules. The dimensions of the hypothetical unit cell resulting from this transformation correspond closely to the average dimensions of the "expanded a" triclinic $Z = 1$ clathrates (see Table IIc).

Figure 11 shows a triclinic $Z = 1$ clathrate with a third type of chain structure. The porphyrin chains in this clathrate exhibit idealized *mmm* symmetry and a repeat distance of about 15 Å. Similar chains extend through the triclinic form of ZnTPP in the *b*-direction. The eugenol clathrate can also be described as an

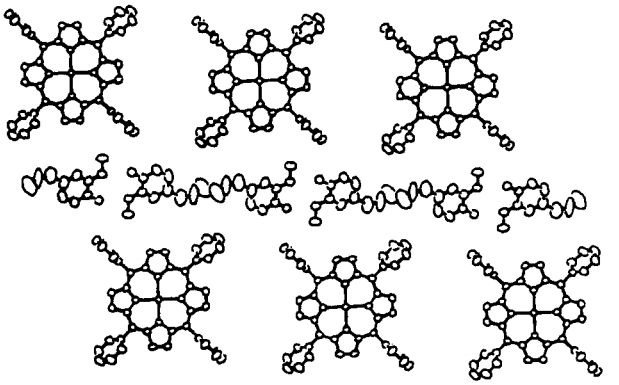

Figure 11. Clathrate with an unusual chain structure.

intercalate of the triclinic structure. In this case the conserved porphyrin sheets are the (1,0,−1) sheets of triclinic ZnTPP. Figure 12 depicts the transformation from the pure host structure to a structure analogous to that of the $Zn^{+2}(eugenol)_2$ clathrate. In this transformation, adjacent sheets are again displaced along the normal to the *ab* plane by *d*(002).

Triclinic $Z = 2$ Clathrates. Most of the 81 triclinic $Z = 2$ clathrates have structures that are closely related to those of the triclinic $Z = 1$ clathrates. The reduction in symmetry associated with the doubling of the unit-cell volume takes a number of different forms. For 21 of these materials, one observes stage 1 intercalate structures very similar to those observed for the $Z =$

(12) Scheidt, W. R.; Mondal, J. U.; Eigenbrot, C. W.; Adler, A.; Radonovich, L. J.; Hoard, J. L. *Inorg. Chem.* **1986**, *25*, 795–799.

(13) The unit cell used to describe the ZnTPP structure herein is that chosen in ref 1c.

Table III. Lattice Parameters for Triclinic $Z = 2$ Clathrates[a]

metal	guest	a	b	c	α	β	γ	vol	d(002)	SG	ref
				a. Stage 1: "Normal"							
Zn^{+2}	N-methylTPP(Cl^-)(CH_2Cl_2)$_{0.66}$	13.467	18.006	11.970	55.25	64.12	54.64	1920	4.855	$P\bar{1}$	CMPORZ[14]
Zn^{+2}	(linalool)	13.355	17.512	16.178	66.67	37.49	69.77	(2111)	4.810	$P\bar{1}$	10
Zn^{+2}	TPB(pyridine)benzene	13.333	17.945	11.452	54.86	75.13	72.97	2129	4.653	$P\bar{1}$	PRPHZN[15]
Zn^{+2}	TPC(pyridine)benzene	13.335	18.032	11.414	54.99	74.92	72.80	2133	4.643	$P\bar{1}$	HPORZN[16]
Zn^{+2}	*N*-benzylTPP(Cl^-)(CH_3CN)$_2$	13.626	19.343	10.579	66.42	59.57	76.61	(2202)	4.294	$P\bar{1}$	FIMHOY[17]
Fe^{+3}	($B_{11}CH_{12}^-$)toluene	13.660	18.839	13.143	50.82	70.37	87.50	2403	4.672	$P\bar{1}$	DOPBAL[18]
Cd^{+2}	(4-picoline)$_3$	13.499	20.743	12.593	72.64	55.99	58.88	2502	5.219	$P\bar{1}$	this work
Fe^{+3}	(pentamethylene sulfide)$_2$(ClO_4^-)($CHCl_3$)$_2$	13.253	25.715	16.724	46.97	43.33	63.75	2842	4.649	$P\bar{1}$	Soltis[19]
hypothetical		13.440	21.251	13.590	51.28	60.37	71.57	2633	4.848		
				b. Stage 1: "Expanded a"							
Zn^{+2}	(trimedlure)	15.030	22.777	15.326	36.28	47.20	50.91	(2236)	4.208	$P\bar{1}$	10
Mo^{+2}	TTP(NO)$_2$benzene	16.607	23.232	20.347	26.37	40.03	46.78	2243	3.989	$P\bar{1}$	DNSPMO[20]
Mg^{+2}	(H_2O)(picoline)$_3$	17.695	25.327	20.648	31.65	29.74	42.84	2408	3.952	$P\bar{1}$	DUJKUO[21]
Zn^{+2}	TDCPP(*N*-Me-pyrrolidinone)$_3$	15.150	22.723	13.155	60.58	47.17	63.65	2850	4.619	$P\bar{1}$	GAMBOL[22]
Zn^{+2}	T(*p*-*n*-octyl)PP	16.081	30.741	10.398	58.37	55.07	54.72	3293	4.080	$P\bar{1}$	GAPJAI[23]
Zn^{+2}	T(*p*-*O*-*n*-octyl)PP(THF)$_2$	19.036	23.345	12.395	62.31	51.66	70.33	3817	4.560	$P\bar{1}$	this work
hypothetical		15.018	26.247	16.899	43.39	34.57	52.52	2596	4.149		
				c. Stage 1: "Two-Channel" "Normal"							
Zn^{+2}	(benzaldehyde)$_2$	13.359	38.130	44.333	44.42	30.67	71.72	(4353)	4.500	$I\bar{1}$	this work
Cd^{+2}	(piperidine)(*o*-xylene)	13.505	36.665	30.688	48.62	32.94	73.72	4587	4.826	$I\bar{1}$	DOFXOL[24]
Co^{+2}	(1,2-dimethylimidazole)(benzene)$_2$	13.611	42.868	36.367	40.01	30.50	64.74	4841	4.587	$I\bar{1}$	DMIPCO[25]
				d. Stage 1: "Two Channel": "Expanded a"							
Ru^{+2}	TDCPP(CO)(styrene oxide)(benzene)$_2$	14.870	38.175	26.486	26.19	61.87	65.29	(5853)	5.675	$I\bar{1}$	SEKZIR[26]
Co^{+3}	(F_4PhS^-)$_2Na^+$kryptate($PhCl$)$_{0.5}$	14.807	57.919	30.463	25.03	43.60	56.82	7074	4.928	$I\bar{1}$	COSJUP[27]
				e. Stage 1: "Doubled a"							
Zn^{+2}	(methyl 4-nitrobenzoate)$_2$	27.086	27.516	21.548	41.17	23.99	62.08	2460	1.868	$P\bar{1}$	this work
Zn^{+2}	(dibenzosuberone)$_3$	29.199	35.088	25.923	14.35	31.99	38.68	3312	2.586	$P\bar{1}$	this work
				f. "Layered"							
Rh^{+3}	(benzyl isocyano)(dibenzaminecarbene)(PF_6^-)	13.269	16.425	14.387	77.31	72.17	80.49	2896	6.736	$P\bar{1}$	JAFXAP[28]
Ce^{+4}	(phthalocyanine)[b]($SbCl_6^-$)	13.568	19.636	20.795	55.68	51.35	50.86	3222	7.796	$P\bar{1}$	SACNUF[29]
Fe^{+3}	(4-Me-imidazolate$^-$)$_2$(K^+kryptate)(toluene)	14.683	24.305	16.879	45.05	54.70	63.48	3472	5.436	$P\bar{1}$	CELWIZ[30]

[a] The unit cells chosen for the materials in sections a and b are analogous to those chosen for the $Z = 1$ materials. The unit cell chosen for the "two-channel" materials in sections c and d have *a* and *b* axes chosen in an analogous fashion, but the *c* axis lies in the porphyrin sheet. For the materials in section e, the *a* axis corresponds to the porphyrin chains, but because of the nature of the cell doubling, it is not possible to choose *b* and *c* in a manner analogous to the other materials without introducing nonstandard translational symmetry. For section f, the *a* axis corresponds to a chain direction and the *ab* plane corresponds to the layers. [b] This is the $SbCl_6^-$ salt of the TPP-Ce-phthalocyanine cation radical.

1 clathrates. For 35 others, stage 2 intercalate structures are observed. These materials contain sheets of guest molecules separated by *double* sheets of porphyrin molecules. For a few of the $Z = 2$ clathrates, one observes an intercalate structure containing layers of *coplanar* porphyrin molecules separated by layers of guest molecules. A final group of clathrates adopt structures which are based on two crystallographically independent half-molecules. These structures, which will not be discussed here, are more closely related to those of the monoclinic clathrates (*vide infra*).

A. Stage 1 Intercalates. The structural relationship between the $Z = 1$ and $Z = 2$ stage 1 intercalates is most easily described in terms of the primitive unit cell for the $Z = 1$ materials shown in Figure 13a. This unit cell has the same *a* and *b* axes as the body-centered cell ordinarily chosen to describe these materials. The third axis, labeled *c'*, lies along a body diagonal of the body-centered cell. The doubling of the unit-cell volume for the stage 1 $Z = 2$ materials is found to correspond to doubling of one of the three axes, *a*, *b*, or *c'*.

Figure 13b represents the symmetry of 14 clathrates tabulated in Table IIIa and b. This structure is characterized by the loss of inversion centers in the porphyrin chains and in the channels and by a doubling of the *c'* axis.

Figure 13c represents the symmetry of 5 clathrates tabulated in Tables IIIc and d. In this structure the inversion centers in the porphyrin chains are lost, but those in the channels are retained. In this case it is the *b* axis that is doubled.

For the $Z = 2$ materials whose lattice parameters are given in Table IIIe, the unit cell is doubled in the *a* direction. In the projection down *a*, the symmetry of these materials is the same as that represented in Figure 13a.

It should be noted that, in all three variations of the stage 1 $Z = 2$ structure, inversion centers relating adjacent chains in a porphyrin sheet are retained and inversion centers in the porphyrin molecules are lost. The loss of molecular inversion symmetry allows an ordered arrangement of five-coordinate porphyrin complexes. Indeed, most of the stage 1 $Z = 2$ materials contain

(14) Lavallee, D. K.; Kopelove, A. B.; Anderson, O. P. *J. Am. Chem. Soc.*, **1978**, *100*, 3025–3033.
(15) Barkigia, K. M.; Fajer, J.; Spaulding, L. D.; Williams, G. J. B. *J. Am. Chem. Soc.* **1981**, *103*, 176–181.
(16) Spaulding, L. D.; Andrews, L. C.; Williams, G. J. B. *J. Am. Chem. Soc.* **1977**, *99*, 6918–6923.
(17) Schauer, C. K.; Anderson, O. P.; Lavallee, D. K.; Battioni, J. P.; Mansuy, D. *J. Am. Chem. Soc.* **1987**, *109*, 3922–3928.
(18) Gupta, G. P.; Lang, G.; Lee, Y. J.; Scheidt, W. R.; Shelly, K.; Reed, C. A. *Inorg. Chem.* **1987**, *26*, 3022–3030.
(19) Soltis, M. Ph.D. Thesis, UCLA, 1988.
(20) Diebold, T.; Schappacher, M.; Chevrier, B.; Weiss, R. *J. Chem. Soc., Chem. Commun.* **1979**, 693–694.
(21) Choon, O. C.; McKee, V.; Rodley, G. A. *Inorg. Chim. Acta* **1986**, *123*, L11–L14.
(22) Williamson, M. M.; Prosser-McCartha, C. M.; Mukundan, S., Jr.; Hill, C. L. *Inorg. Chem.* **1988**, *27*, 1061–1068.
(23) Chiaroni, A.; Riche, C.; Bied-Charreton, C.; Dubois, J. C. *Acta Crystallogr., Sect. C* **1988**, *44*, 429–432.
(24) Rodesiler, P. F.; Griffith, E. A. H.; Charles, N. G.; Lebioda, L.; Amma, E. L. *Inorg. Chem.* **1985**, *24*, 4595–4600.
(25) Dwyer, P. N.; Madura, P.; Scheidt, W. R. *J. Am. Chem. Soc.* **1974**, *96*, 4815–4819.
(26) Groves, J. T.; Han, Y.; Van Engen, D. *J. Chem. Soc., Chem. Commun.* **1990**, 436–437.
(27) Doppelt, P.; Fischer, J.; Weiss, R. *J. Am. Chem. Soc.*, **1984**, *106*, 5188–5193.
(28) Boschi, T.; Licoccia, S.; Paolesse, R.; Tagliatesta, P.; Pelizzi, G.; Vitali, F. *Organometallics* **1989**, *8*, 330–336.
(29) Lachkar, M.; De Cian, A.; Fischer, J.; Weiss, R. *New J. Chem.* **1988**, *12*, 729–731.
(30) Quinn, R.; Strouse, C. E.; Valentine, J. S. *Inorg. Chem.* **1983**, *22*, 3934–3940.

Table IV. Lattice Parameters for Triclinic $Z = 2$ Clathrates (stage 2)

metal	guest	*a*	*b*	*c*	α	β	γ	vol	*d*(002)[b]	SG	ref
				a. Stage 2: "Normal"							
Mn^{+3}	$(H_2O)(F_3CSO_3^-)$	13.049	33.925	30.111	52.63	32.43	78.61	3828	4.411	$P\bar{1}$	FAVTOL[31]
Fe^{+3}	(benzenethiolate$^-$)	13.415	34.156	20.811	27.65	68.05	78.26	3919	4.368	$P\bar{1}$	1b
Zn^{+2}	(4-chlorophenol)	13.435	32.279	21.491	25.98	76.49	80.91	(3940)	4.600	$P\bar{1}$	this work
Zn^{+2}	$(pyrazine)_{1.5}$	13.464	31.684	19.272	31.66	72.57	80.37	4053	4.818	$P\bar{1}$	this work
U^{+4}	$(Cl^-)_2(THF)$	13.419	36.298	19.490	28.63	69.60	80.31	4058	4.226	$P\bar{1}$	FEBVIR[32]
Fe^{+2}	(nitrosyl)(4-Me-piperidine)	13.448	31.148	19.924	31.91	71.76	81.18	4084	4.933	$P\bar{1}$	NIPORF[33]
Zn^{+2}	(4-methylcyclohexanone)	13.539	31.164	20.316	29.61	76.07	81.01	4086	4.902	$P\bar{1}$	this work
Cu^{+2}	$[TPP^{\bullet+}](SbCl_6^-)$	13.926	35.895	13.486	41.66	73.03	67.26	4132	4.482	$P\bar{1}$	BOSBAM[34]
Zn^{+2}	(hexanol)	13.385	34.864	24.093	25.01	65.64	74.68	4150	4.611	$P\bar{1}$	10
Zn^{+2}	(6-Me-5-hepten-2-ol)	13.342	34.682	24.075	25.92	65.99	75.38	4265	4.763	$P\bar{1}$	10
Fe^{+3}	(phenyl$^-$)pentane	13.330	39.407	22.834	65.82	27.20	80.99	4336	4.179	$P\bar{1}$	CUHXAE[35]
Zn^{+2}	(grandlure III/IV)	13.253	34.786	23.818	27.29	63.69	73.13	4367	4.950	$P\bar{1}$	10
Zn^{+2}	(grandlure II)	13.263	35.186	24.345	26.69	62.94	71.65	(4423)	4.993	$P\bar{1}$	10
Zn^{+2}	(phenethyl propionate)	13.440	36.543	23.919	25.18	66.09	74.28	4428	4.683	$P\bar{1}$	10
hypothetical		13.440	34.266	23.366	25.52	73.29	78.69	4387	4.858		
				b. "Head-On"							
Co^{+2}	*N*-methylTPP(Cl^-)	14.971	27.754	30.950	43.43	34.49	70.07	3751	4.801	$P\bar{1}$	CMPORC[36]
Fe^{+2}	*N*-methylTPP(Cl^-)	14.961	27.933	30.921	43.48	34.61	70.17	3794	4.825	$P\bar{1}$	CPRNFE[37]
Mn^{+2}	*N*-methylTPP(Cl^-)	14.993	27.930	30.972	43.53	34.63	70.25	3808	4.831	$P\bar{1}$	CMPOMN[38]
				c. Stage 2: "Expanded a"							
Zn^{+2}	(3-nitroaniline)	14.943	35.492	27.944	47.40	24.38	62.31	3900	4.152	$P\bar{1}$	this work
Zn^{+2}	(5-octanoic lactone)	14.937	38.145	26.221	26.28	39.29	53.59	(3912)	4.266	$P\bar{1}$	this work
Zn^{+2}	(2,5-hexanedione)	15.361	39.151	27.671	25.37	37.15	51.81	3958	4.187	$P\bar{1}$	this work
Mg^{+2}	$(2\text{-propanol})_2$	14.961	36.950	24.120	25.51	48.20	60.43	(4032)	4.192	$P\bar{1}$	this work
Fe^{+3}	$(bicycloheptene\text{-}CO_2^-)(benzene)_{0.5}$	14.822	34.350	20.903	27.31	59.73	67.78	(4151)	4.404	$P\bar{1}$	this work
Fe^{+2}	(4-Cl-Ph-vinylidenecarbene)	14.739	42.707	30.088	20.60	46.60	56.49	(4525)	4.310	$P\bar{1}$	GAMCAY[39]
hypothetical		15.018	40.962	28.872	22.73	42.41	55.21	4192	4.149	$P\bar{1}$	
				d. Stage 2: "Zig-Zag"[a]							
Nb^{+5}	$(oxo^{-2})(acetate^-)$(acetic acid)	18.591	25.349	11.867	62.26	118.33	61.89	1999	4.809	$P\bar{1}$	NBPOAC[40]
Mg^{+2}	$(H_2O)(acetone)_2$	18.967	33.006	12.926	49.20	110.23	64.00	(2034)	3.616	$P\bar{1}$	GEPBUY[41]
Ni^{+2}	$(N\text{-tosylamino})CH_2Cl_2$	19.136	38.807	14.378	47.06	89.04	44.52	2226	4.275	$P\bar{1}$	TSAPNI[42]
Mo^{+6}	$TTP(oxo^{-2})_2$(toluene)	20.035	28.664	13.129	61.28	116.19	59.02	2274	4.618	$P\bar{1}$	OTPHMO[43]
Ru^{+2}	(CO)(pyridine)$(toluene)_{1.5}$	19.670	31.559	10.759	43.33	87.78	52.57	2447	4.964	$P\bar{1}$	TPPCRU[44]
Sn^{+2}	$(Hg\text{-}Mn_2(CO)_9)(CH_2Cl_2)_{0.5}$	19.672	36.704	14.792	20.02	60.07	49.99	2566	4.639	$P\bar{1}$	TPMNSN[45]
hypothetical		19.007	34.256	10.673	42.19	90.00	56.31	2632	4.857	$P\bar{1}$	
				e. Stage 2: "Hybrid"							
W^{+6}	$(oxo^{-2})(peroxo^{-2})$(benzene)	13.046	30.692	14.923	46.38	63.95	68.36	3866	5.194	$P\bar{1}$	DAWDOU[46]
Zn^{+2}	(anthrone)	12.799	41.865	22.509	25.77	54.02	57.98	4243	4.670	$P\bar{1}$	this work
Zn^{+2}	(9-xanthone)	12.850	41.810	22.788	25.54	54.02	58.31	4271	4.671	$P\bar{1}$	this work
Au^{+3}	$(Pt^{+2}(mnt^{-2})_2)_{0.5}$	14.990	38.942	22.527	37.23	33.34	59.85	3811	3.774	$P\bar{1}$	GAFTAI[47]
Ni^{+2}	*N*-ethoxycarbonylcarbeneTPP($CHCl_3$)	16.666	37.634	24.968	28.13	36.56	52.90	4078	4.076	$P\bar{1}$	ECTPNI[48]
Fe^{+3}	$(Cu^{+2}(mnt^{-2})_2)_{0.5}(THF)_{2.5}$	17.687	33.760	33.753	61.49	29.48	86.37	5058	4.244	$P\bar{1}$	FUPGEC[49]

[a] The primitive unit cell chosen for the "zig-zag" structures has the same *a* and *b* axes as the body-centered cells chosen for many of the other clathrates, but the *c* axis is chosen to lie in the porphyrin sheet. [b] *d*(001) for the "zig-zig" structures.

five-coordinate complexes. More detailed descriptions of each of the three subclasses of this group follow.

The $Z = 2$ clathrates whose structures correspond to that in Figure 13b are shown in Figures 14 and 15. These figures reflect the loss of inversion symmetry in the channel. The tetrakis(4-octylphenyl)porphinatozinc structure (Figure 15) is not formally a clathrate, but its structure is similar to an "expanded a" clathrate, with the octyl side chains of the porphyrin molecule acting as guests.

Figures 16 and 17 show clathrates whose host structures correspond to that in Figure 13c. Doubling of the *b* axis results in the formation of two crystallographically distinct channels. Viewed as intercalates, each layer of guest molecules consists of alternating channels of the two types. These "two-channel" structures occur with both "normal" and "expanded a" porphyrin chains. In these clathrates, the inversion centers in the channel are retained and those in the porphyrin chains are lost.

Figure 18 shows two $Z = 2$ clathrates that exhibit a doubling of the unit cell along the porphyrin chain direction. The Zn^{+2}-(dibenzosuberone)$_3$ clathrate exhibits a chain structure very similar to that of the ZnTPP(eugenol)$_2$ clathrate in Figure 11.

B. Stage 2 Intercalates. Included in the triclinic $Z = 2$ clathrates are 34 materials that exhibit stage 2 intercalate structures in which sheets of guest molecules are separated by double sheets of host molecules. Figure 19 shows structures for 14 "normal" stage 2 clathrates. Lattice parameters for these materials are compiled in Table IVa. As in the stage 1 intercalates, the "normal" lattice is characterized by chains which exhibit the perpendicular arrangement of interacting phenyl groups and by a 13.5 Å repeat distance. The perpendicular arrangement of

(31) Williamson, M. M.; Hill, C. L. *Inorg. Chem.* **1986**, *25*, 4668–4671.
(32) Girolami, G. S.; Milam, S. N.; Suslick, K. S. *Inorg. Chem.* **1987**, *26*, 343–344.
(33) Scheidt, W. R.; Brinegar, A. C.; Ferro, E. B.; Kirner, J. F. *J. Am. Chem. Soc.* **1977**, *99*, 7315–7322.
(34) Scholz, W. F.; Reed, C. A.; Lee, Y. J.; Scheidt, W. R.; Lang, G. *J. Am. Chem. Soc.* **1982**, *104*, 6791–6793.
(35) Doppelt, P. *Inorg. Chem.* **1984**, *23*, 4009–4011, and personal communication.
(36) Anderson, O. P.; Lavallee, D. K. *J. Am. Chem. Soc.* **1977**, *99*, 1404–1409.
(37) Anderson, O. P.; Kopelove, A. B.; Lavallee, D. K. *Inorg. Chem.* **1980**, *19*, 2101–2107.
(38) Anderson, O. P.; Lavallee, D. K. *Inorg. Chem.* **1977**, *16*, 1634–1640.
(39) Mansuy, D.; Battioni, J. P.; Lavallee, D. K.; Fischer, J.; Weiss, R. *Inorg. Chem.* **1988**, *27*, 1052–1056.
(40) Lecomte, C.; Protas, J.; Guilard, R.; Fliniaux, B.; Fournari, P. *J. Chem. Soc., Dalton Trans.* **1979**, 1306–1313.
(41) McKee, V.; Rodley, G. A. *Inorg. Chim. Acta* **1988**, *151*, 233–236.
(42) Callot, H. J.; Chevrier, B.; Weiss, R. *J. Am. Chem. Soc.* **1978**, *100*, 4733–4741.
(43) Mentzen, B. F.; Bonnet, M. C.; Ledon, H. J. *Inorg. Chem.* **1980**, *19*, 2061–2066.
(44) Little, R. G.; Ibers, J. A. *J. Am. Chem. Soc.* **1973**, *93*, 8583–8590.
(45) Onaka, S.; Kondo, Y.; Yamashita, M.; Tatematsu, Y.; Kato, Y.; Goto, M.; Ito, T. *Inorg. Chem.* **1985**, *24*, 1070–1076.
(46) Yang, C. H.; Dzugan, S. J.; Goedken, V. L. *J. Chem. Soc., Chem. Commun.* **1985**, 1425–1426.
(47) Zhong, Z. J.; Nishida, Y.; Okawa, H.; Kida, S. *Mem. Fac. Sci., Kyushu Univ. Ser. C* **1987**, *16*, 19–24.
(48) Chevrier, B.; Weiss, R. *J. Am. Chem. Soc.* **1976**, *98*, 2985–2990.
(49) Serr, B. R.; Headford, C. E. L.; Elliott, C. M.; Anderson, O. P. *J. Chem. Soc., Chem. Commun.* **1988**, 92–94.

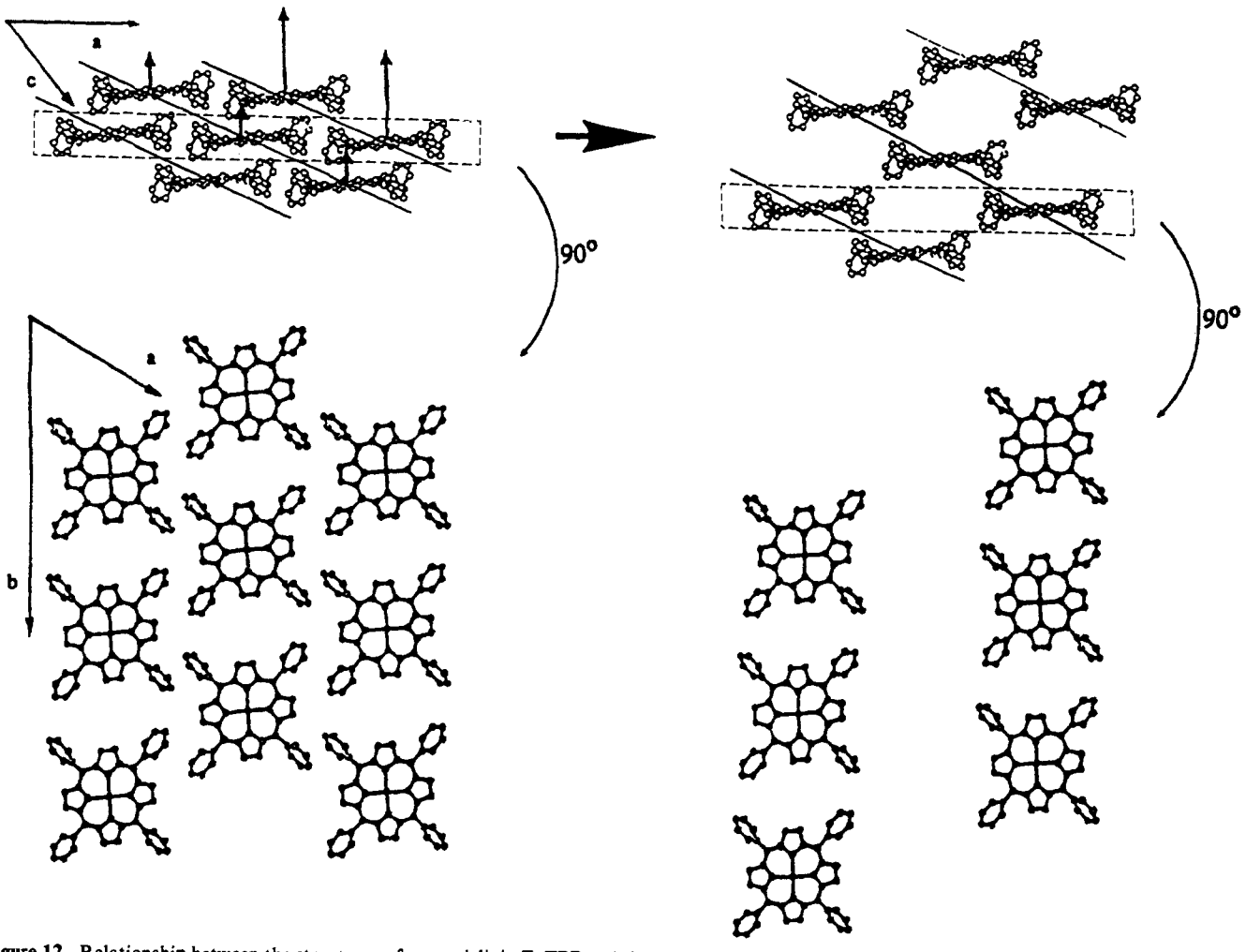

Figure 12. Relationship between the structures of pure triclinic ZnTPP and the ZnTPP (eugenol)$_2$ clathrate. Adjacent sheets are displaced along the normal to the *ab* plane by *d*(002).

phenyl groups is also seen between porphyrin molecules in adjacent coplanar chains. This produces the same "pin-wheel" arrangement of phenyl groups as is observed in the I4/m host structure (see Figure 2).

Figure 20 depicts the transformation of the I4/m host structure to the "normal" stage 2 clathrate structure. As in the stage 1 materials, (0,1,1) sheets are conserved. In the stage 2 transformation, pairs of adjacent sheets are displaced by $c/2$ relative to neighboring pairs. The lattice parameters of the hypothetical transformed unit cell correspond closely to the lattice parameters of the "normal" stage 2 clathrates (Table IVa).

Stage 2 "expanded a" structures are shown in Figure 21. The porphyrin chains in these structures exhibit the parallel arrangement of phenyl groups and the 15 Å porphyrin–porphyrin repeat distance found in the stage 1 "expanded a" clathrates. The interaction between porphyrin chains in the double layer is also of the parallel type. The double chains in these materials are very similar to those found in triclinic ZnTPP.

Figure 22 depicts the transformation of the triclinic ZnTPP structure to the stage 2 "expanded a" structure. As in the transformation to the stage 1 lattice, (0,2,2) sheets are conserved. In the stage 2 materials, however, *pairs* of adjacent sheets are displaced by *d*(002) along the normal to the *ab* plane. The lattice parameters of the hypothetical unit cell compare well to the parameters of the clathrate unit cells (Table IVc).

A third type of porphyrin lattice has been observed among the stage 2 triclinic $Z = 2$ structures which does not have an analog among the stage 1 structures. These "zig-zag" structures (Figure 23) are composed of porphyrin chains which exhibit a repeat distance of ca. 19 Å. The double porphyrin chains characteristic

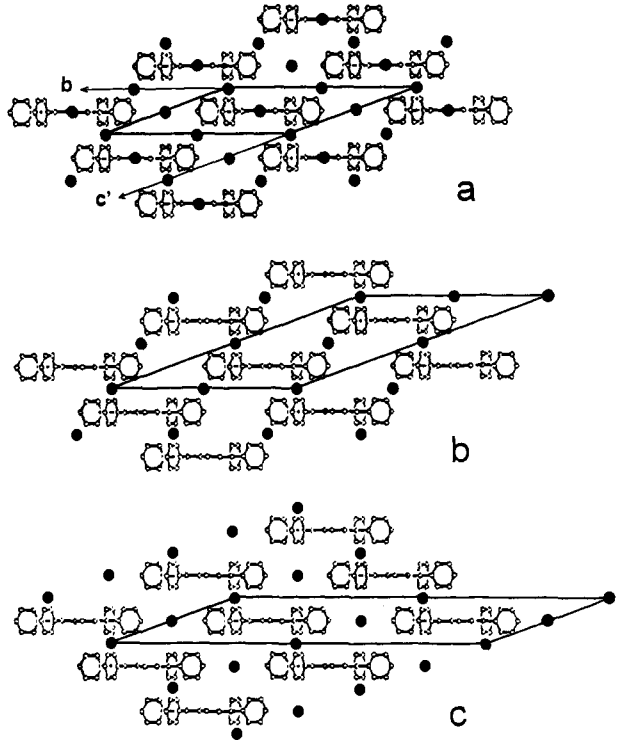

Figure 13. (a) $Z = 1$ host structure viewed down the *a* axis. The filled circles indicate the location of inversion centers. (b) $Z = 2$ host structure in which the primitive unit cell is doubled in the *c'* direction. (c) $Z = 2$ host structure in which the unit cell is doubled along the *b* direction.

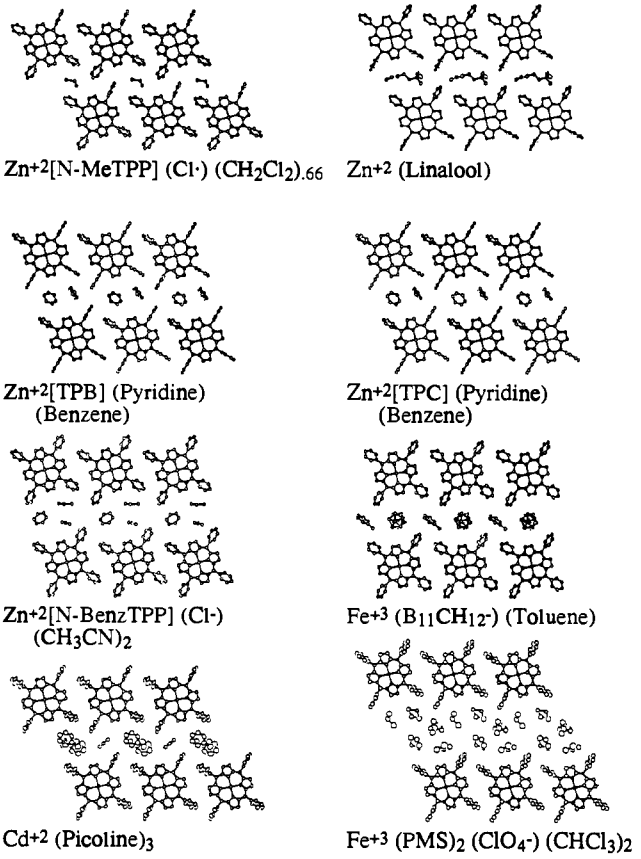

Figure 14. "Normal" $Z = 2$ stage 1 clathrates.

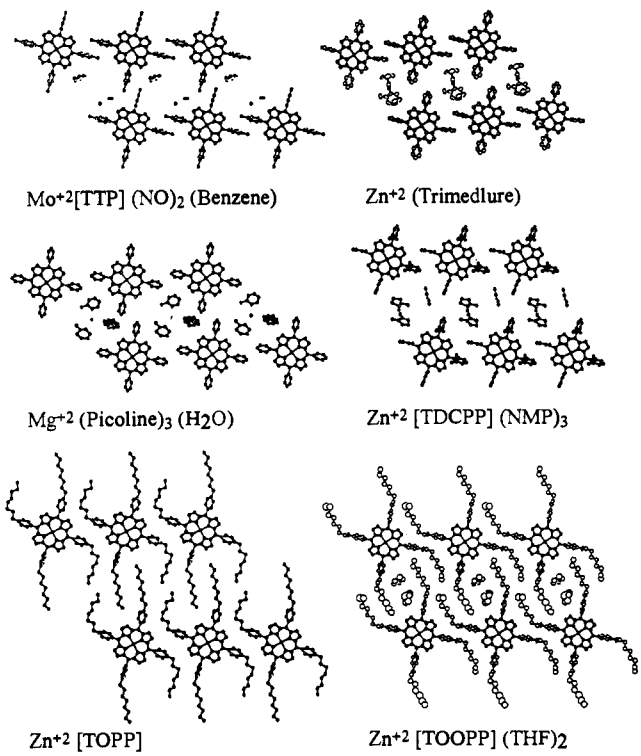

Figure 15. "Expanded a" $Z = 2$ stage 1 clathrates.

of the "zig-zag" structures are similar to those which extend through the I4/m structure in the [1,1,0] direction. In the transformation shown in Figure 24, the clathrate lattice structure is seen to result when pairs of (1,–1,2) porphyrin sheets are separated from adjacent pairs by $c/2$. The lattice parameters of the hypothetical transformed unit cell correspond reasonably well to the lattice parameters of the "zig-zag" clathrates (Table IVd).

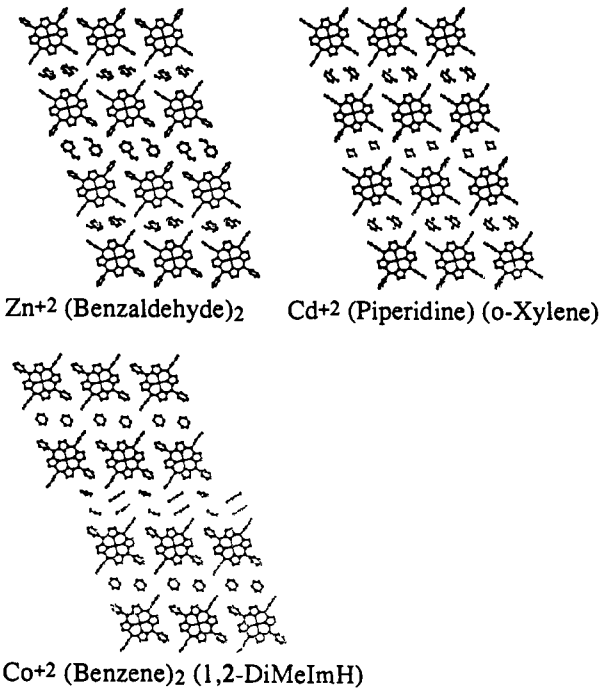

Figure 16. "Normal" $Z = 2$ "two-channel" clathrates.

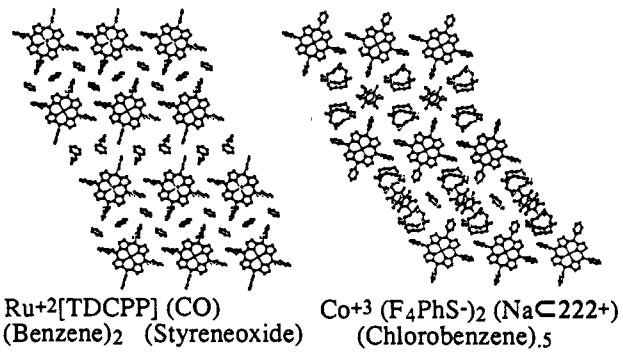

Figure 17. "Expanded a" $Z = 2$ "two-channel" clathrates.

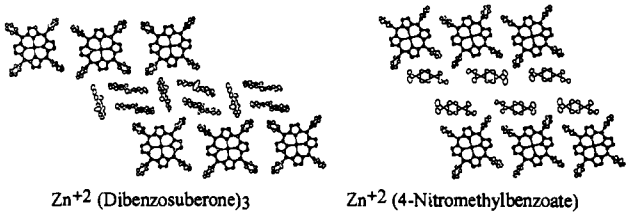

Figure 18. Stage 1 $Z = 2$ clathrates with a doubling of the unit cell in the chain direction.

Three isostructural *N*-methyl-substituted porphyrins (Table IV) represented by the manganese complex in Figure 25 contain chains of porphyrin molecules similar to those seen in the eugenol and dibenzosuberone clathrates. These materials have a sheared structure characteristic of the stage 2 intercalates, but the double sheets in these materials differ significantly from those in triclinic ZnTPP, perhaps because of the methyl substitution of the porphyrin.

Figure 26 shows stage 2 triclinic $Z = 2$ structures which exhibit both parallel and perpendicular interactions between molecules in the double chain. In anthrone, xanthone, and benzene clathrates, the extended chains exhibit perpendicular interactions with parallel interactions between the two components of the double chain. On the other hand, in the $Pt(mnt)_2$ clathrate the extended chains are of the parallel type, with perpendicular interactions between the two components of the double chain. No pure host material has been found to exhibit these "hybrid" structures.

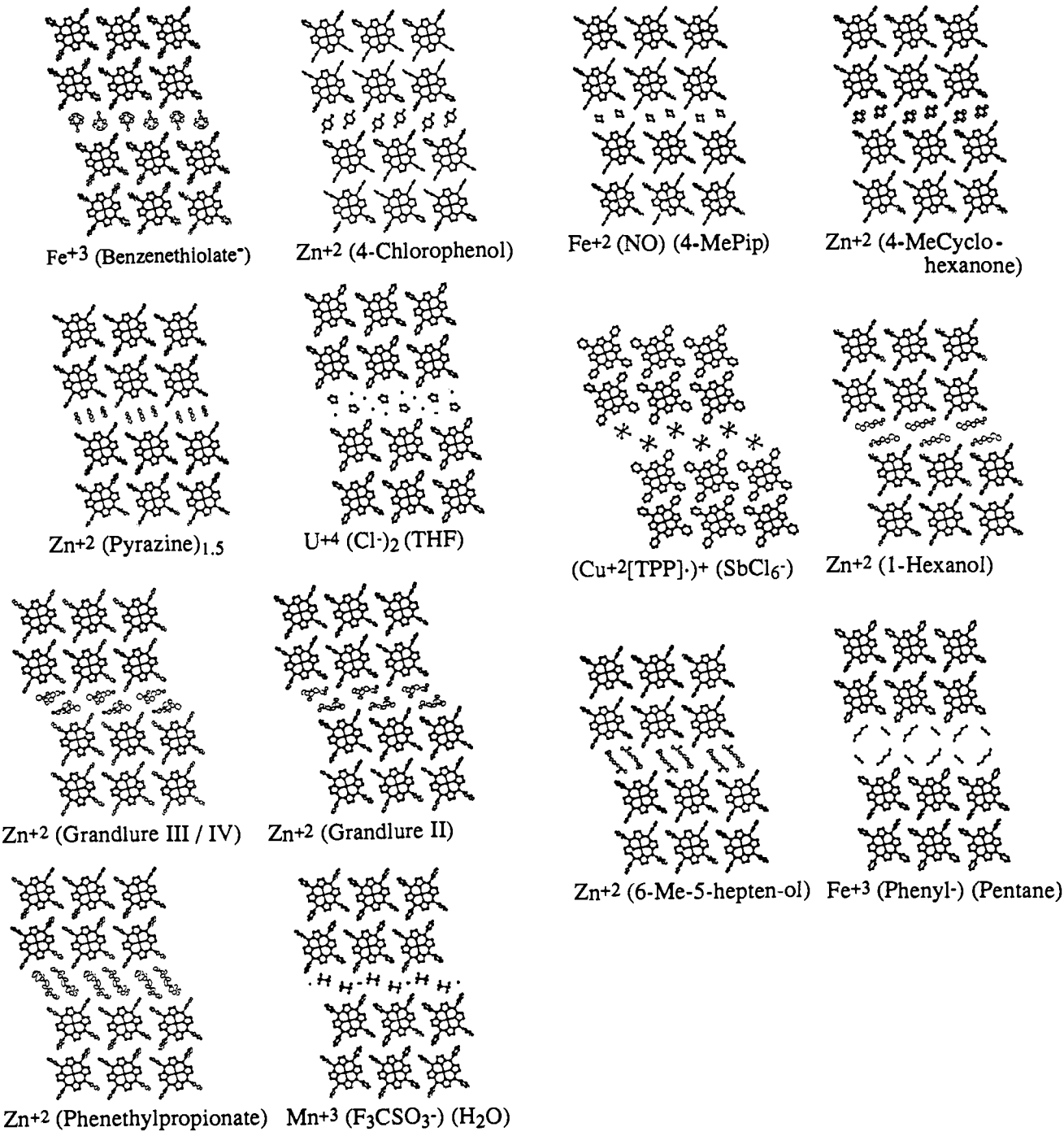

Figure 19. "Normal" stage 2 clathrates.

Intercalates with Layers of Coplanar Host Molecules. A few porphyrin-based clathrates adopt structures that are best described as containing layers of *coplanar* porphyrin molecules separated by layers of guests. Lattice parameters for four such "layered" materials are tabulated in Tables IIe and IIIf, and their structures are represented in Figure 27. Like the more common intercalate structures described above, these materials exhibit staging. The four materials shown in Figure 27 exhibit three different arrangements of host and guest layers. The Zn clathrate contains alternating single layers, while the Fe and Rh clathrates contain double layers of host molecules separated by single layers of guest molecules. (In the drawing of the Fe clathrate, the double layer is shown, while, for the Rh clathrate, only a single layer is shown.) The Ce clathrate contains double layers of host molecules separated by double layers of guest molecules. The host layers in these materials share a number of structural features with the clathrates described previously. For example, the Rh and Zn clathrates contain "normal" chains of porphyrin molecules, while the other two contain "expanded a" chains. As a group, these materials are distinguished by having guest molecules which are comparable in size to the host molecules.

Monoclinic Z = 2 Clathrates. The porphyrin lattice structures observed among the monoclinic porphyrin clathrates with two porphyrin molecules in the primitive unit cell show a number of features similar to those of the triclinic clathrates. Chains of translationally equivalent, co-planar porphyrin molecules extend through the crystal in one dimension. Four neighboring chains outline a channel in which the guest species reside. The monoclinic structures differ from the triclinic structures in that adjacent chains are not translationally equivalent but are related to each other by two-fold symmetry operations.

In Figure 28 the two most common monoclinic porphyrin lattice structures are compared to the triclinic $Z = 1$ lattice. The basic features of the monoclinic lattices may be view as being derived

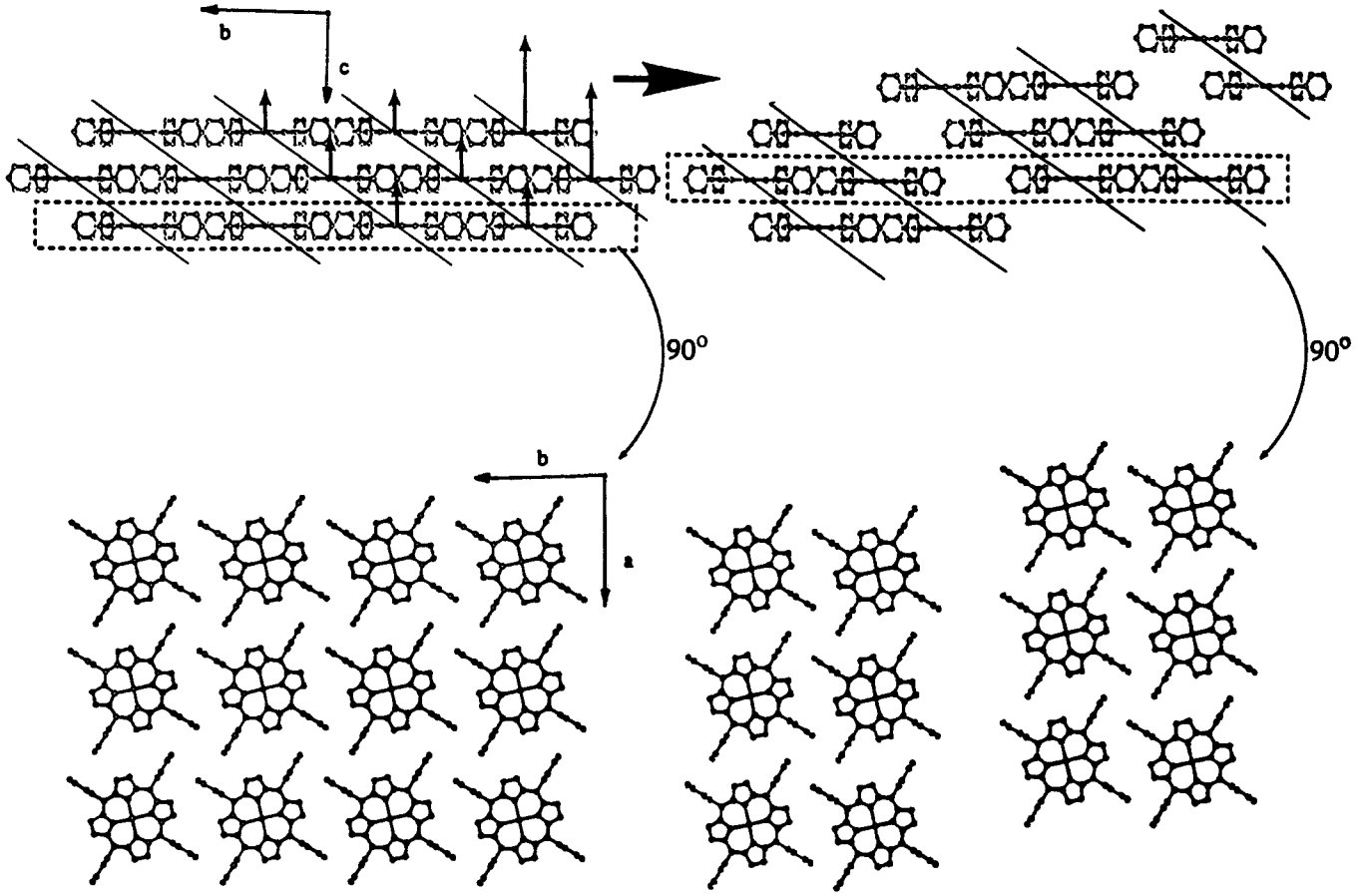

Figure 20. Transformation of the I4/m structure to the stage 2 "normal" structure.

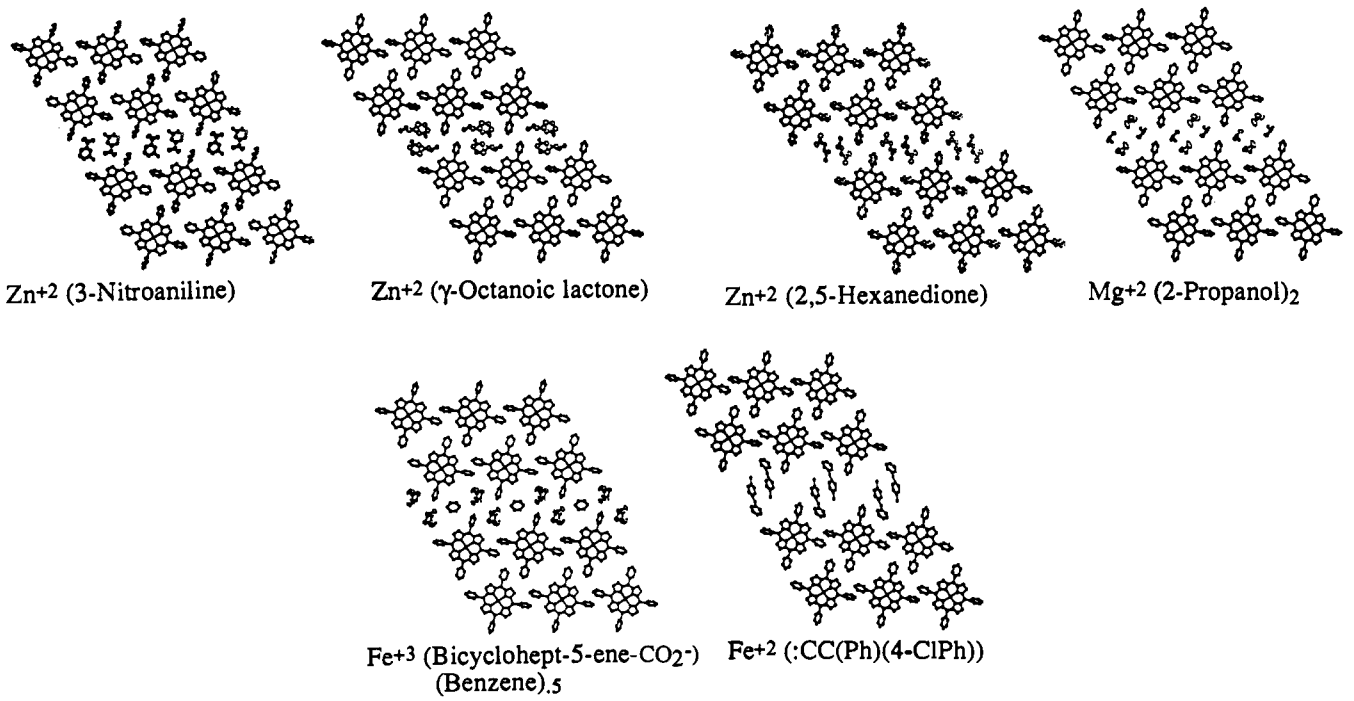

Figure 21. Stage 2 "expanded a" clathrates.

from the triclinic lattice by simple rotations. The lattice depicted in Figure 28b, can be derived from the triclinic lattice (Figure 28a) by application of a two-fold rotation to alternate (0,1,0) layers. This operation disrupts the sheet structure of the triclinic clathrates and yields a "herring-bone" array of porphyrin chains. In most cases this transformation is accompanied by a significant increase in the repeat distance in the porphyrin chains. The lattice pictured in Figure 28c can be derived from the triclinic lattice by a two-fold rotation of alternate (0,1,1) layers. In this case, the basic sheet structure typical of the triclinic clathrates is retained.

Figures 29 and 30 show 28 monoclinic $Z = 2$ "herring-bone" clathrates. As was the case in the triclinic clathrates, different lattice types can be distinguished among the "herring-bone" structures by the nature of the porphyrin–porphyrin interaction within the chains. In the most common chain structure observed

Table V. Lattice Parameters for Monoclinic and Orthorhombic Clathrates

metal	guest	SG	a	b	c	β	vol	φ	ref
		a. $Z = 2$ "Herring-Bone" Clathrates with 19 Å Chain Structures							
Fe^{+3}	$(NO)(H_2O)(ClO_4^-)$	$P2_1/n$	21.367	8.124	10.304	82.23	1772	84.5	CILKUD[50]
Fe^{+3}	$(H_2O)_2(ClO_4^-)$	$P2_1/n$	21.670	8.136	10.415	82.70	1821	65.0	51
Mn^{+3}	$(ClO_4^-)(H_2O)_2$	$P2_1/n$	21.359	8.193	10.523	84.46	1833	66.4	FUWGEJ[52]
Fe^{+3}	$TPP^+(ClO_4^-)_2$	$P2_1/n$	22.714	14.662	12.131	152.79	1847	51.7	BUBFAF10[53]
$2H^+$	TTP	$P2_1/n$	20.994	9.287	9.879	99.91	1897	60.8	CUSYIY[54]
Zn^{+2}	(diphenylacetylene)	$P2_1/n$	18.122	15.804	10.536	137.10	(2054)	56.1	this work
Zn^{+2}	$(toluene)_2$	$P2_1/n$	18.212	15.229	10.430	134.23	(2073)	74.3	this work
Cu^{+2}	$(picoline)_2$	$P2_1/n$	18.256	15.372	10.125	133.03	(2077)	81.9	this work
Zn^{+2}	$(benzene)_2$	$P2_1/n$	18.386	15.819	10.867	137.87	2120	57.5	SEMLUR[14]
Zn^{+2}	$(4\text{-fluorobenzaldehyde})_2$	$P2_1/n$	18.851	15.689	10.215	134.04	(2172)	60.2	this work
Cr^{+2}	$(toluene)_2$	$P2_1/n$	18.569	15.777	10.518	134.79	2187	60.1	CRPORT[55]
Fe^{+3}	$(CN^-)_2(K^+)(acetone)_2$	$P2_1/n$	20.283	11.438	9.600	100.78	2188	68.4	KCNPFE[56]
Zn^{+2}	(1,4-diisopropylbenzene)	$P2_1/n$	23.076	10.134	17.633	147.72	2202	121.8	this work
Zn^{+2}	$(1\text{-methyl-}1,4\text{-cyclohexadiene})_2$	$P2_1/n$	18.682	16.239	10.389	134.67	2241	57.2	this work
Zn^{+2}	$(m\text{-toluic acid})_2$	$P2_1/n$	15.822	21.253	10.036	137.00	2302	69.0	this work
Zn^{+2}	$(o\text{-toluic acid})_2$	$P2_1/n$	19.696	16.392	10.981	139.23	(2316)	62.1	this work
Zn^{+2}	$(mesitylene)_2$	$P2_1/n$	17.309	20.282	10.010	137.78	(2362)	63.4	this work
Mo^{+2}	$TTP(pyridine)_4$	$P2_1/n$	18.803	9.221	16.942	110.98	2743	135.5	CIKZAX[57]
		b. "Herring-Bone" Clathrates with Unusual Chain Structures							
Zn^{+2}		$P2_1/n$	14.703	8.898	14.681	118.90	1682	24.9	this work
Co^{+3}	$(formylmethyl^-)$	Pn	24.073	12.750	13.134	154.60	1729	20.2	COTWEN[58]
Mg^{+2}	$(MeOH)_2$	$P2_1/n$	13.302	12.868	11.039	113.29	1736	28.7	GEPBIM[40]
Fe^{+3}	$(EtOH)_2(BF_4^-)$	$P2_1/n$	11.968	16.823	10.560	109.53	2004	58.3	TPFETB[59]
Mg^{+2}	$(MeOH)_2$acetone	$P2_1/n$	13.130	17.755	10.010	65.20	2119	108.8	GEPBOS[40]
Mn^{+3}	$(p\text{-toluate}^-)(p\text{-toluic acid})(H_2O)_2$	$P2_1/n$	13.396	20.528	9.930	68.33	2400	51.7	this work
Zn^{+2}	$(phenethylpropionate)_2$	$P2_1/n$	12.906	26.960	11.066	138.12	(2567)	23.5	10
Zn^{+2}	[bis(hexanediyldioxydiphenylene)porphinato](CHCl$_3$)	$P2_1/n$	13.776	22.212	8.608	88.10	2633	40.2	FIDNUB[60]
Zn^{+2}	$[T(4\text{-OH})PP](xylene)_2(MeOH)_4$	$P2_1/n$	14.666	17.875	12.048	61.99	(2789)	15.6	this work
Fe^{+2}	$[TP(piv)P](Na^+\subset 222)(2\text{-MeIm}^-)$	$P2_1$	13.430	26.165	17.319	125.93	4928	81.4	SIBZIM[61]
		c. $Z = 2$ Clathrates with Sheet Structures							
Zn^{+2}	$T(4\text{-MeO})PP(m\text{-cresol})_2$	$P2_1/a$	15.713	9.675	14.672	98.53	2206		1c
Mg^{+2}	$(acetophenone)_2$	$P2_1/a$	13.508	20.653	10.819	129.23	2338		this work
Co^{+2}	$((R)\text{-phenethylamine})_2$	$P2_1$	13.509	20.506	11.083	129.27	2377		this work
Mg^{+2}	$((R)\text{-phenethylamine})_2$	$P2_1$	13.522	20.583	11.135	129.47	2392		this work
Zn^{+2}	$((S)\text{-phenethylamine})_2$	$P2_1$	13.563	20.606	11.083	129.11	2403		this work
Zn^{+2}	$(4\text{-thiocyanatonitrobenzene})_2$	$P2_1/a$	13.390	19.375	11.986	128.51	2433		this work
Zn^{+2}	$(trans\text{-anethole})_2$	$P2_1/a$	13.256	21.261	11.855	132.62	2459		this work
Zn^{+2}	$(2\text{-methoxy-}3\text{-isobutylpyrazine})_2$	$P2_1/c$	14.774	10.968	21.055	131.50	(2555)		this work
Fe^{+1}	$(Na^+dibenzo\text{-}18\text{-crown-}6)(THF)_2$	$P2_1/m$	12.796	21.864	12.108	103.47	3294		FTPBZC10[62]
		d. $Z = 4$ Clathrates							
Zn^{+2}	(3-penten-2-ol)	$P2_1/a$	13.440	35.812	10.553	127.46	4032		this work
Zn^{+2}	(2-phenylethylamine)	$P2_1/a$	13.481	35.499	10.688	127.96	(4033)		this work
Zn^{+2}	(3-methylcyclohexanone)	$P2_1/n$	17.759	18.245	15.405	124.91	4093		10
Zn^{+2}	$(Fe^0(2,4\text{-hexadienal})(CO)_3)_2$	$Pcab$	13.062	18.121	21.984	90.00	5204		this work

among the "herring-bone" clathrates, the porphyrin–porphyrin repeat distance is ca. 19 Å (see Figure 31a). This chain structure is similar to that of the "zig-zag" triclinic $Z = 2$ stage 2 clathrates. Figure 29 depicts the "herring-bone" clathrates that exhibit this chain structure. Lattice parameters for these materials are compiled in Table Va.

The porphyrin chains of the nine "herring-bone" clathrates shown in Figure 30 (and tabulated in Table Vb) differ from those of the clathrates in Figure 29. The porphyrin chains in some of these clathrates exhibit the perpendicular arrangement of phenyl groups and a repeat distance of about 13.5 Å, common to the "normal" triclinic clathrates (see Figure 31c). In other clathrates the chains exhibit the "head-on" arrangement of phenyl groups and a repeat distance of about 15 Å (see Figure 31b), similar to those of the $ZnTPP(eugenol)_2$ clathrate. Notably, the guest species among these monoclinical clathrates include a disproportionate number of smaller molecules and/or noncoordinated anions.

The monoclinic $Z = 2$ structures which exhibit the porphyrin sheet structure are depicted in Figure 32, and their lattice parameters are compiled in Table Vc. In most cases, the sheets are similar to those of the "normal" stage 1 triclinic clathrates in that they are formed by the step-wise layering of chains which exhibit the perpendicular orientation of interacting phenyl groups and a 13.5 Å repeat distance. The guest species are incorporated in layers between the sheets.

Monoclinic and Orthorhombic $Z = 4$ Clathrates. Structural analysis of porphyrin-based lattice clathrates is currently being extended to include those clathrates that crystallize with monoclinic symmetry and contain four porphyrin molecules in the primitive unit cell (monoclinic $Z = 4$) as well as to those with higher symmetry. A number of these structures have already been found to exhibit features very similar to those discussed in the previous examples. Figure 33 shows one orthorhombic and three monoclinic $Z = 4$ porphyrin clathrate structures. Lattice parameters for these materials are compiled in Table Vd. These materials exhibit single- and double-sheet structures very similar to those found for the triclinic clathrates.

(50) Scheidt, W. R.; Lee, Y. J.; Hatano, K. *J. Am. Chem. Soc.* **1984**, *106*, 3191–3198.
(51) Keder, N. Ph.D. Thesis, UCLA, 1984.
(52) Williamson, M. M.; Hill, C. L. *Inorg. Chem.* **1987**, *26*, 4155–4160.
(53) Gans, P.; Buisson, G.; Duee, E.; Marchon, J. C.; Erler, B. S.; Scholz, W. F.; Reed, C. A. *J. Am. Chem. Soc.* **1986**, *108*, 1223–1234.
(54) Butcher, R. J.; Jameson, G. B.; Storm, C. B. *J. Am. Chem. Soc.* **1985**, *107*, 2978–2980.
(55) Scheidt, W. R.; Reed, C. A. *Inorg. Chem.* **1978**, *17*, 710–714.
(56) Scheidt, W. R.; Haller, K. J.; Hatano, K. *J. Am. Chem. Soc.* **1980**, *102*, 3017–3021.
(57) Colin, J.; Strich, A.; Schappacher, M.; Chevrier, B.; Veillard, A.; Weiss, R. *Nouv. J. Chim.* **1984**, *8*, 55–64.
(58) Masuda, H.; Taga, T.; Sugimoto, H.; Mori, M. *J. Organomet. Chem.* **1984**, *273*, 385–392.
(59) Gans, P.; Buisson, G.; Duee, E.; Regnard, J. R.; Marchon, J. C. *J. Chem. Soc., Chem. Commun.* **1979**, 393–395.
(60) Simonis, U.; Walker, F. A.; Lee, P. L.; Hanquet, B. J.; Meyerhoff, D. J.; Scheidt, W. R. *J. Am. Chem. Soc.* **1987**, *109*, 2659–2668.
(61) Mandon, D.; Ott-Woelfel, F.; Fischer, J.; Weiss, R.; Bill, E.; Trautwein, A. X. *Inorg. Chem.* **1990**, *29*, 2442–2447.
(62) Mashiko, T.; Reed, C. A.; Haller, K. J.; Scheidt, W. R. *Inorg. Chem.* **1984**, *23*, 3192–3196.

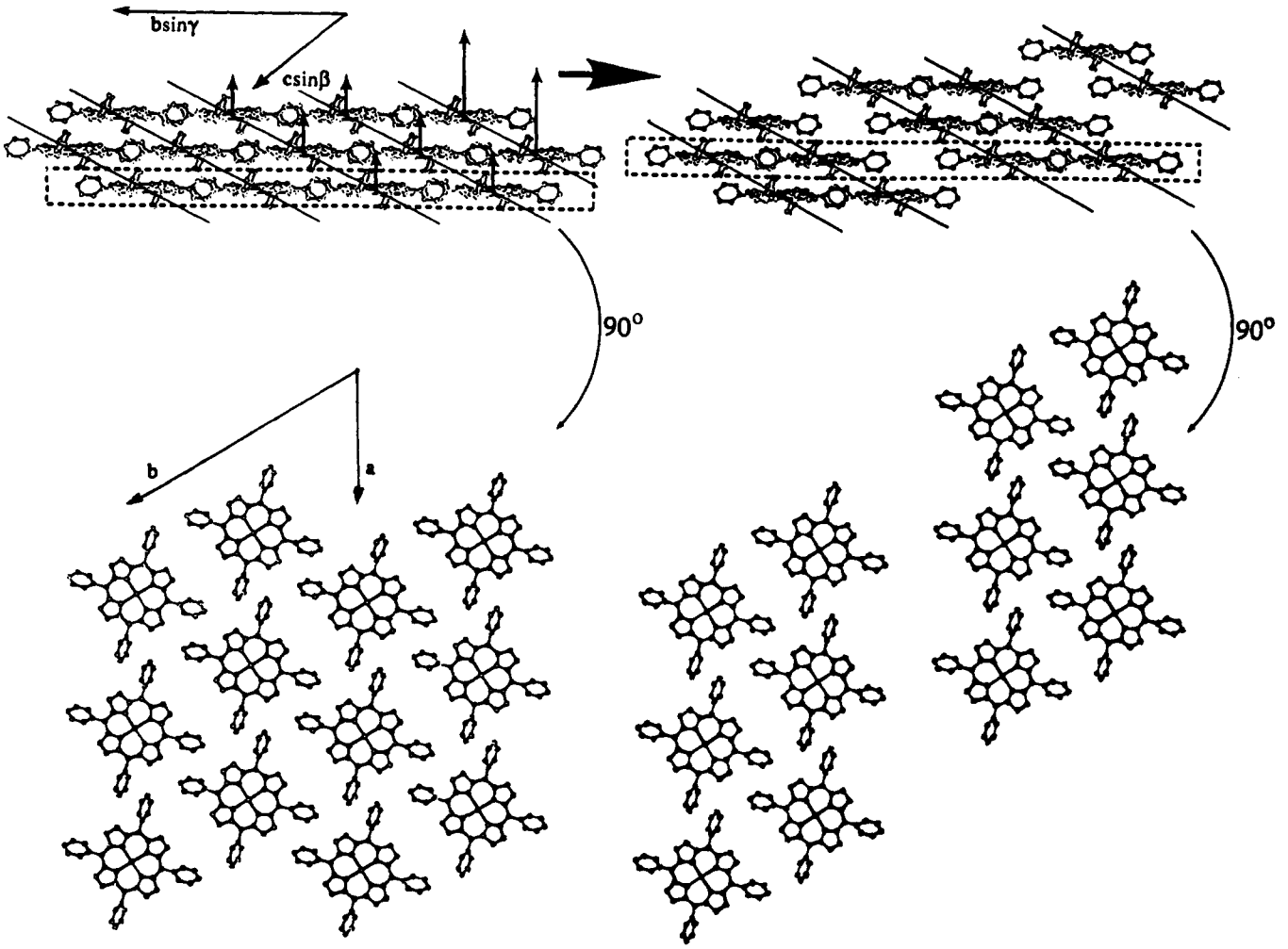

Figure 22. Transformation from the triclinic ZnTPP structure to the stage 2 "expanded a" structure.

Discussion

One approach to the rational construction of crystalline solids is based on the design of molecular building blocks that self-assemble in a prescribed fashion. Analyses of the structures of a large number of porphyrin-based clathrates demonstrate that the tetraphenylporphyrin molecule serves as an excellent prototype of such a building block. Although the TPP molecule lacks any functionality that might be expected to dictate the relative disposition of neighboring molecules, one finds that the host structure is strongly conserved in porphyrin-based clathrates. This conservation, together with the extensive structural database provided in this and in previous reports, allows the prediction of clathrate structure for a wide range of guest species on a purely empirical basis. Modern molecular modeling techniques can be used to extend and refine these empirical predictions.

The large majority of porphyrin-based clathrates exhibit crystal structures in which sheets of porphyrin molecules separate sheets of guest molecules. These clathrates can best be viewed as arising from different modes of intercalation. The relative displacement of adjacent sheets of host molecules provides the freedom necessary to accommodate guests of widely varying size, shape, and composition. The lack of covalent or hydrogen-bonding interactions between host molecules imparts a degree of flexibility to the sheet structure that also contributes to the versatility of these hosts. A common characteristic of intercalate structures is the occurrence of staging. The observation of a large number of stage 2 "porphyrin sponges" further demonstrates the appropriateness and utility of the intercalate description.

The structural analyses reported herein focused on triclinic and monoclinic clathrates. The new triclinic $Z = 1$ clathrates exhibit structures closely related to a large number described previously. These new materials further document the diversity of guest species that can be accommodated by porphyrin-based

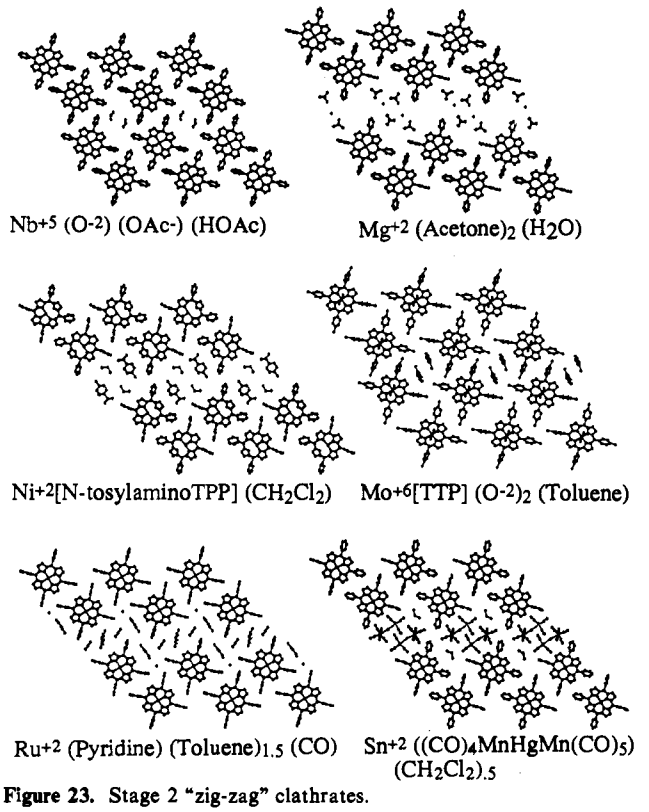

Figure 23. Stage 2 "zig-zag" clathrates.

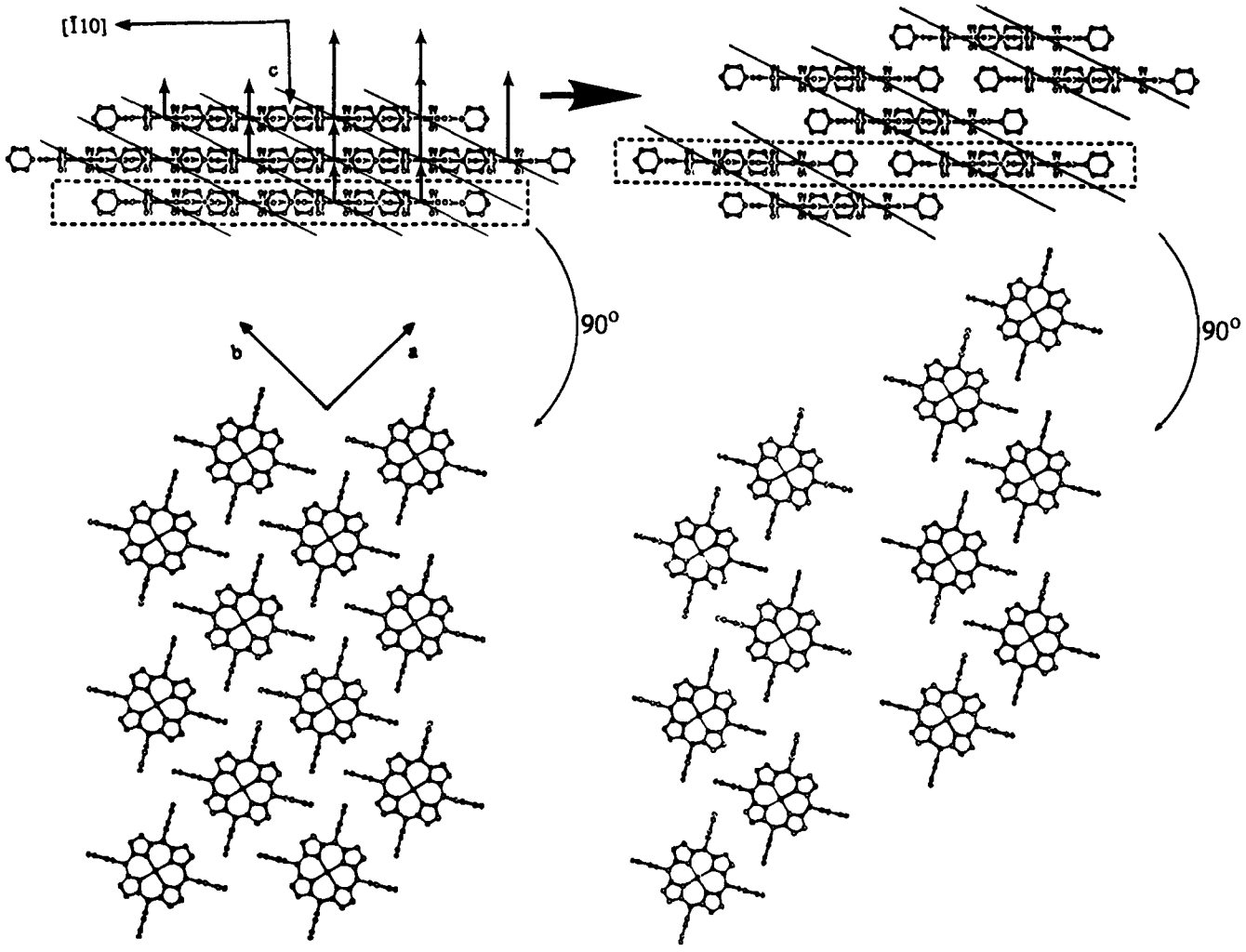

Figure 24. Transformation from the I4/m structure to the stage 2 "zig-zag" structure.

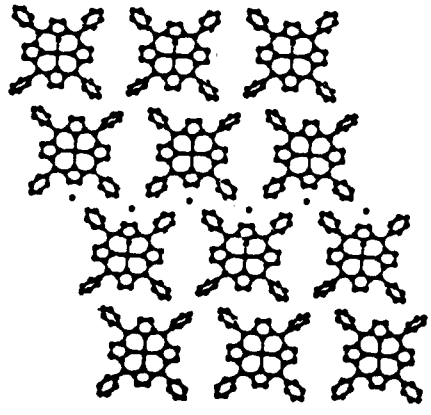

Mn^{+2}[N-MeTPP](Cl^-)

Figure 25. Stage 2 clathrate with "head-on" chain structure.

hosts. Examination of the structural systematics of triclinic $Z = 2$ clathrates reveals that the reduction in symmetry associated with the cell doubling can take a number of different forms. These include stage 1 and stage 2 structures, both of which can be described as arising from shear distortions of pure host materials. A different type of intercalation is observed for a few clathrates with very large guests. In these materials, layers of coplanar porphyrin molecules separate layers of guest molecules.

An examination of all available monoclinic $Z = 2$ porphyrin-based clathrate structures has revealed two predominant structural types. Both types contain one-dimensional porphyrin chains similar to those seen in the triclinic clathrates. In one type, the two-dimensional sheet structure characteristic of the triclinic clathrates is also preserved. Finally, in a selection of monoclinic $Z = 4$ and higher symmetry clathrates, one again sees the conservation of single and double porphyrin sheets. There are, however, a large number of monoclinic $Z = 4$ materials in which the sheet structure is not conserved.

The large base of structural information available for the porphyrin-based clathrates offers some generalization concerning those factors that influence adoption of the various closely related clathrate structures. In the most common structure, the stage 1 intercalate, the host molecule site is either centrosymmetric or pseudo-centrosymmetric. On the other hand, in the stage 2 intercalates, the symmetry of the host molecule site is broken by formation of the double host layers. As a result, anything that destroys the symmetry of the host molecule favors the adoption of stage 2 intercalates. For example, if the host molecule forms a stable five-coordinate complex with a stoichiometric amount of ligating guest, and if no additional guest species is available to fill a pseudoinversion-related guest site, the resulting clathrate is likely to adopt the stage 2 structure. A good example of this is Fe(III)TPP(benzenethiolate). This molecule has been crystallized[1b] from toluene, chlorobenzene, and benzenethiol with the formation of triclinic stage 1 clathrates in which a solvent molecule occupies a site pseudoinversion related to the benzenethiolate ligand. If, however, it is crystallized from a small-molecule solvent that does not tend to incorporate, this material crystallizes with a stage 2 structure. Most of the stage 2 intercalates involve five-coordinate complexes. Formation of a clathrate in which the host species is a monoanion and the guest species is a dication also dictates a low symmetry at the host site.

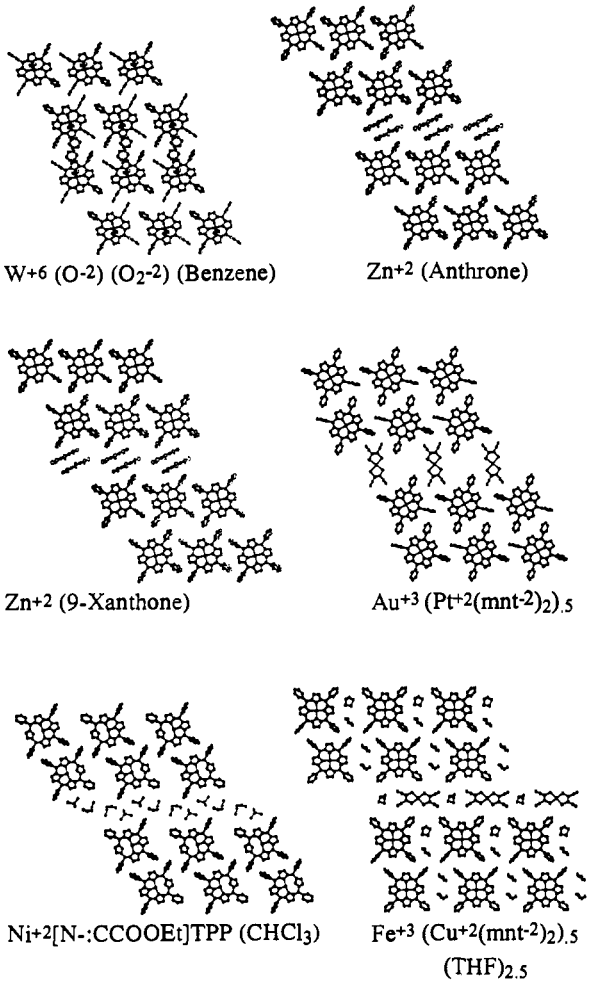

Figure 26. Stage 2 "Hybrid" clathrates.

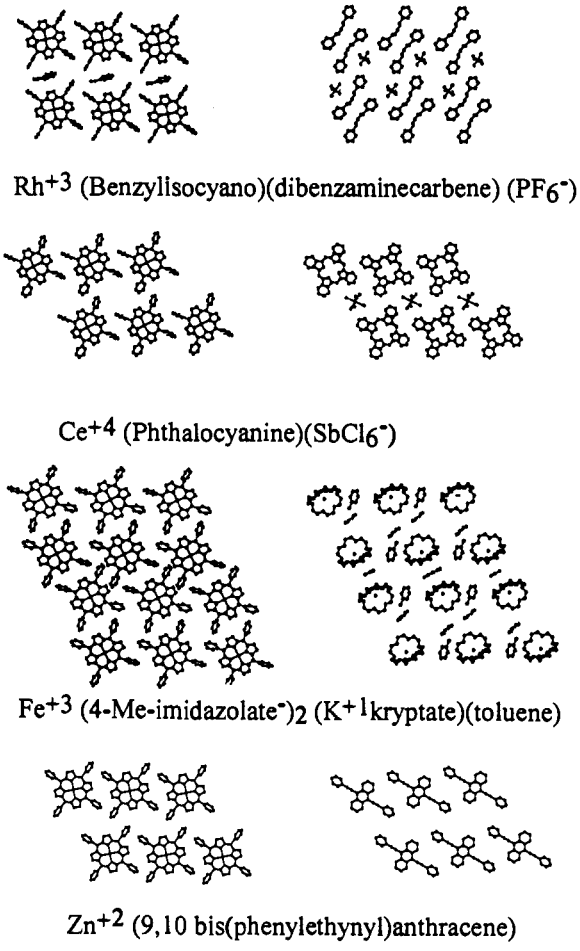

Figure 27. "Layered" clathrates. For each material, the drawing on the left shows the host layer and the drawing on the right the guest layer.

Overall, the monoclinic $Z = 2$ structures are far less common than the triclinic structures. Smaller guests appear to favor adoption of the monoclinic structure, but it is difficult to identify any other guest characteristic associated with this structural type.

Any variation in clathrate structure dictated by the guest species represents a limitation on the utility of the porphyrin building blocks for lattice design. On the other hand, it was found previously[1c] that in some cases seeding can produce crystals of a desired structure even though that structure is not the most thermodynamically stable. The large base of structural information available for these clathrates can be used to select appropriate seed materials for this type of lattice construction.

Most of the new porphyrin-based clathrates reported herein were prepared in conjunction with the development of various scientific and technological applications of these materials. Included are several clathrates that contain insect attractants. These were prepared to study the potential of porphyrin-based clathrates as controlled-release substrates. A description of the thermodynamic and kinetic studies of guest release from these materials will be reported elsewhere. A large number of fused-ring organics were incorporated into ZnTPP to explore the influence of guest size and shape on clathrate structure. The new clathrates also included several containing organometallic guests. Use of porphyrin-based hosts to crystallize and stabilize organometallic complexes may prove to have some general utility. Finally, several of these clathrates were prepared in conjunction with studies of molecular separation and solid-state reactivity.

The investigation of structural systematics of porphyrin-based clathrates bears a symbiotic relationship to the development of practical applications of these materials. Structural determinations carried out in conjunction with the development work have provided an extensive database in which it is possible to recognize structural regularities. In turn, examination of the structural systematic allows one to identify those aspects of the structure that can be modified to better accommodate a particular

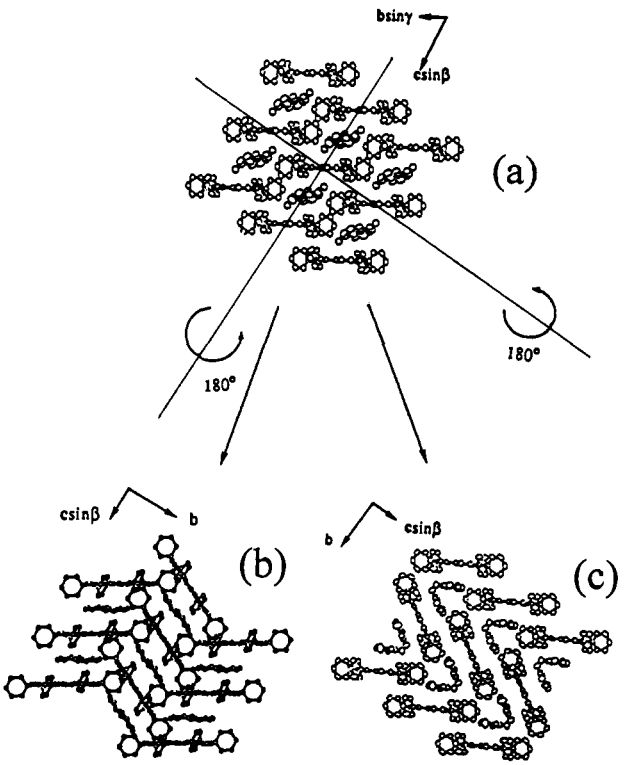

Figure 28. Relationship between triclinic and monoclinic clathrates.

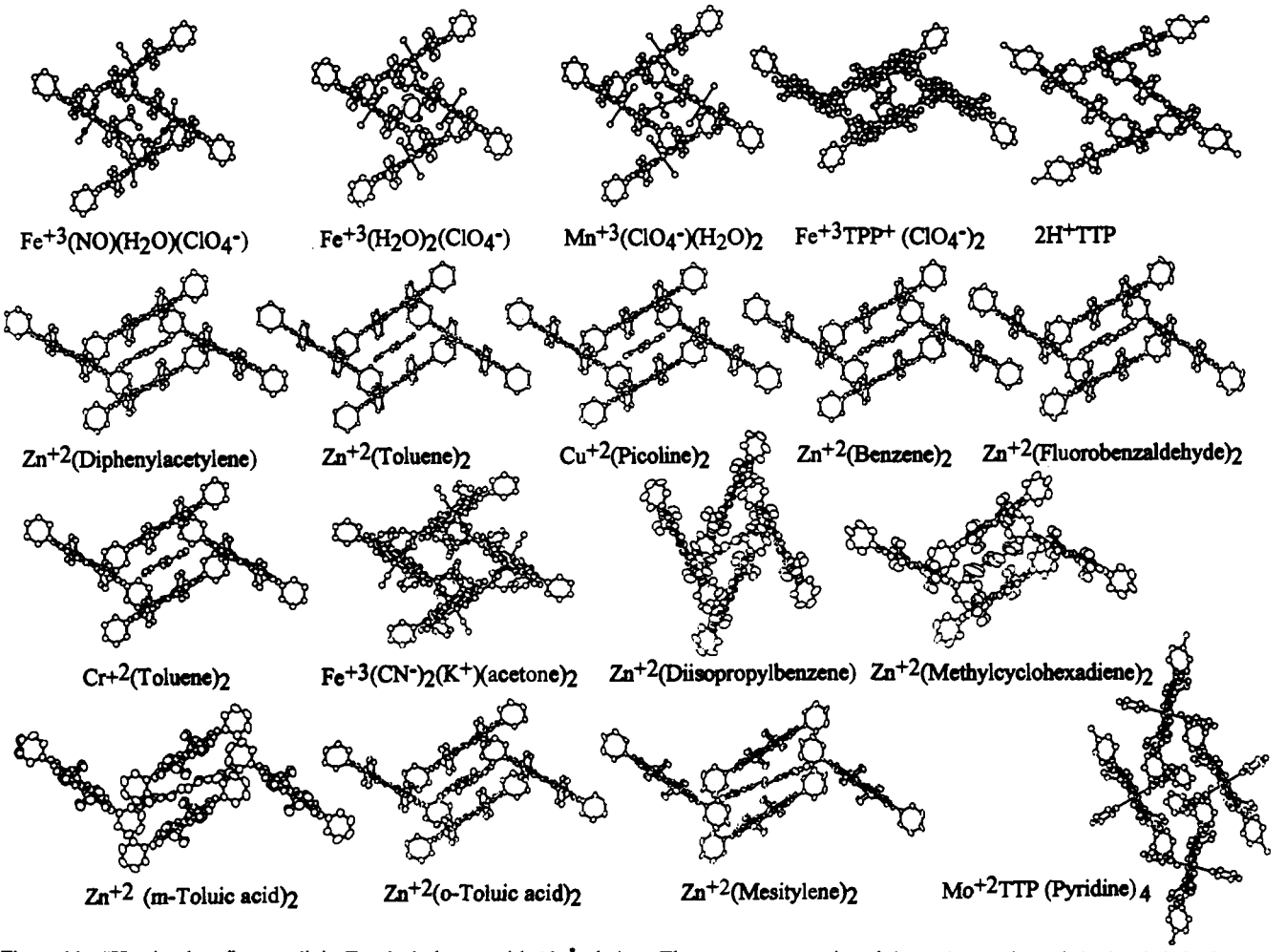

Figure 29. "Herring-bone" monoclinic $Z = 2$ clathrates with 19 Å chains. The structures are viewed down the *a* axis, and the *b* axis is horizontal.

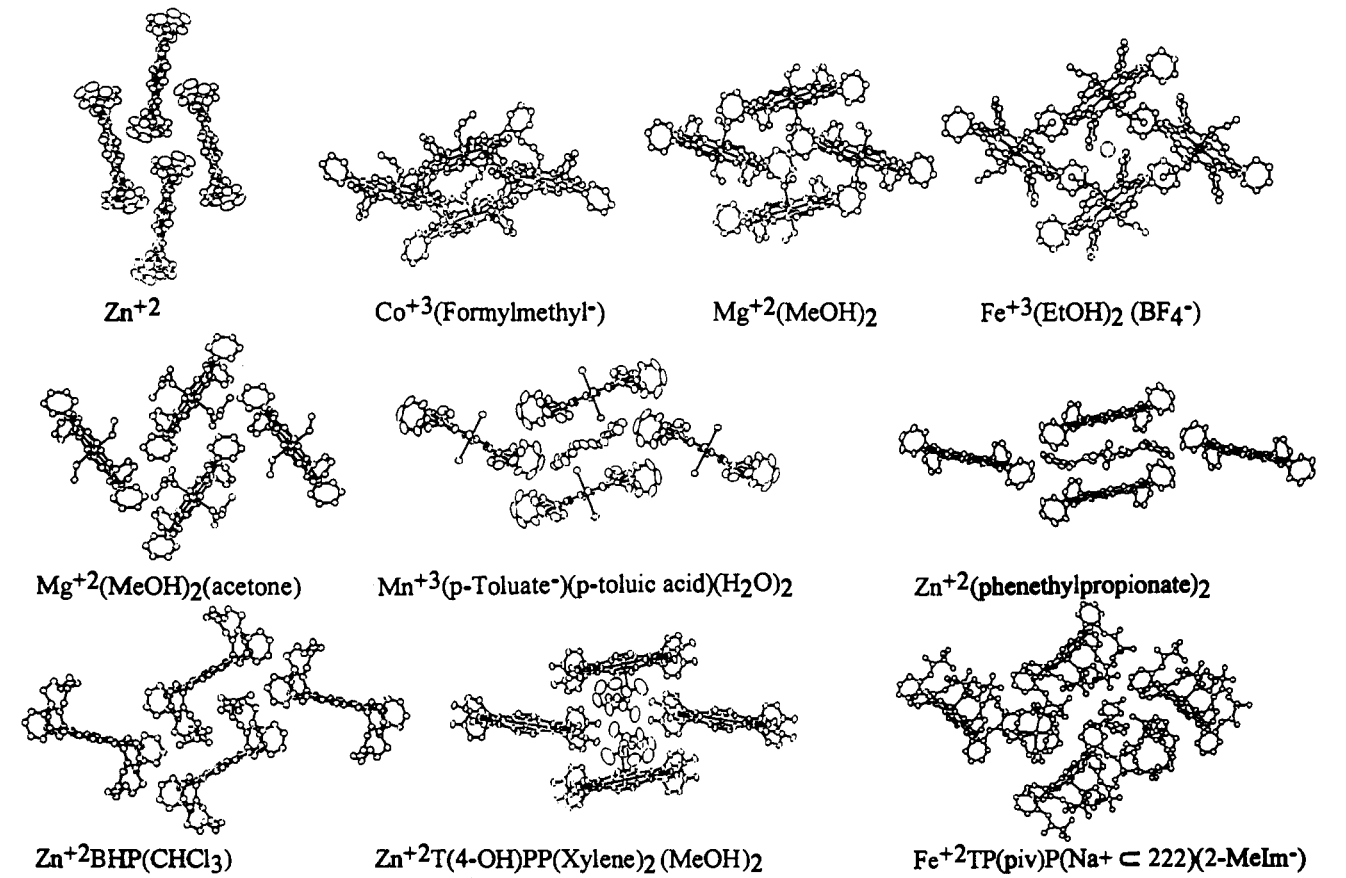

Figure 30. "Herring-bone" clathrates with a variety of chain structures. The structures are viewed down the *a* axis with the *b* axis horizontal.

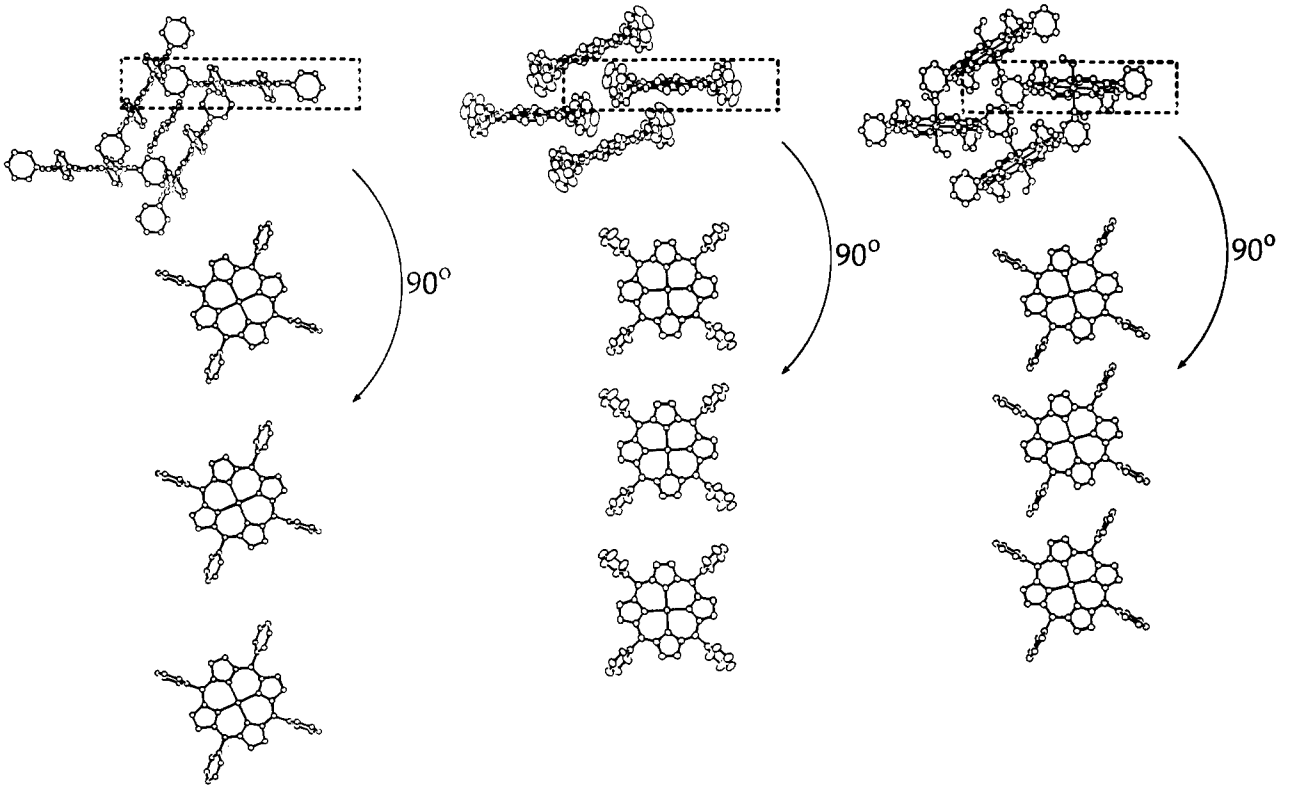

Figure 31. Chain structures of monoclinic clathrates.

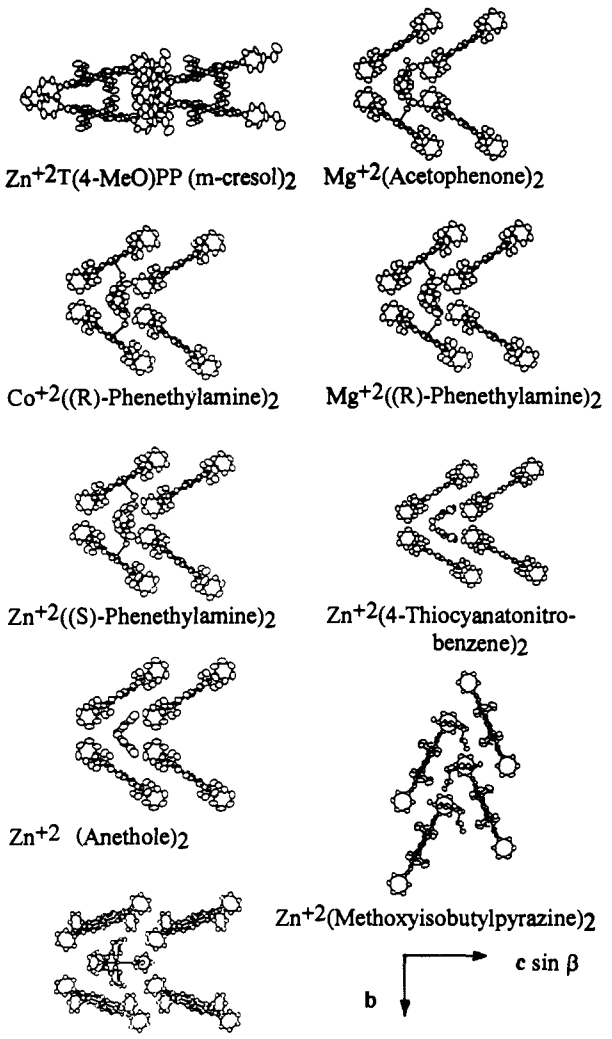

Figure 32. Monoclinic $Z = 2$ clathrates with sheet structures.

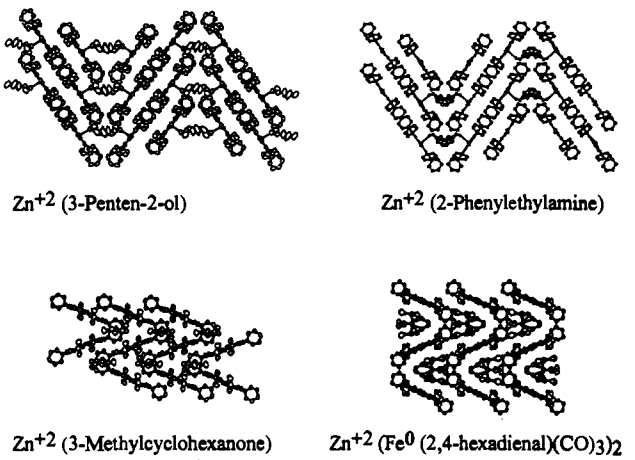

Figure 33. Monoclinic and orthorhombic $Z = 4$ clathrates.

guest molecule or to alter the thermodynamics or kinetics of guest release.

The large body of structural information available for these clathrates will allow the development of detailed and useful models of the crystal packing. Indeed, the availability of a large number of closely related structures should allow the refinement of the methods used in modeling other molecular solids. Molecular modeling efforts now underway are directed both at the rational modification of porphyrin-based hosts for specific applications and at the design of new building blocks for the construction of microporous solids.

Acknowledgment. This work was supported by the National Science Foundation (Grant CHE 9003033), the Frasch Foundation, NATO, and Trece Inc. We thank Mr. Greg Easter for the synthesis of the oxyoctyl-substituted porphyrin and Mr. Eskandar Ensafi for the synthesis of zinc tetraphenylporphyrin.

Supplementary Material Available: Transformation matrices used to convert from the unit cells in which the structures were determined to those chosen herein and a listing of structural parameters for 75 materials (220 pages). Ordering information is given on any current masthead page.